APL TDR 64-87

SOLAR FLAT PLATE THERMOELECTRIC GENERATOR RESEARCH

TECHNICAL DOCUMENTARY REPORT NO. APL TDR 64-87

September 14, 1964

AF Aero Propulsion Laboratory
Research and Technology Division
Air Force Systems Command
Wright-Patterson Air Force Base, Ohio

Project No. 8173, Task No. 817302

(Prepared under Contract AF 33(657)-10335 by
General Instrument Corporation, Thermoelectric Division,
Newark, New Jersey; Robert E. Rush, Author)

FOREWORD

This report was prepared by General Instrument Corporation under USAF Contract AF33(657)-10335, Research and Technology Division, Aero Propulsion Laboratory. Mr. C. Glassburn was the Project Engineer for the Laboratory during the major portion of the program. Captain R. Morrow was Project Engineer during the latter stage of the program.

ABSTRACT

A solar flat plate thermoelectric converter consists of a collector plate with an optically selective coating, small size thermoelements, a radiator plate and a support structure. This report describes the research and development work performed during the 15 month period of this program.

The collector and radiator plates were folded into self-supporting structures which, combined with aluminum tubular members, comprised the panel support configuration. This design resulted in a very low converter weight, only 53 grams per square foot.

A number of prototype panels, both 4" x 4" and 12" x 12" in area were fabricated and tested. The panels passed specified environmental test without physical or electrical changes. These tests included sinusoidal vibration, 14-3000 cps., to 15 g's for 45 minutes in each axis; random vibration, white noise with an amplitude of 0.05 g^2 for 5 minutes in each axis; acceleration, 12 g's in each axis for 10 minutes; and three shocks of 40 g's for 6 milliseconds in each axis. The panels were also subjected to 500 thermal cycles of 1 1/2 hour per cycle. Other panels were subjected to over 6000 thermal cycles without resistance change. This number of thermal cycles is equivalent to one year's operation.

Evaluation of the optically selective coating disclosed that the coating efficiency actually obtained in the pilot production runs was only 80% of the literature value. The processing of the bismuth telluride thermoelectric material into the shape and size required for the solar panels caused a decrease in performance relative to large size thermoelements. This decrease, combined with basic material properties inferior to literature values, resulted in a thermoelectric efficiency only 50% of that initially expected.

The overall panel performance in the Earth orbit operational temperature regime resulted in approximately 11 watts per pound of panel. If thermoelectric properties of microelements used in panels equalled those of larger sizes, almost 18 watts per pound could be attained. Additional engineering effort to obtain properties given in the literature for thermoelectric materials and optical coatings could result in panels providing almost 30 watts per pound.

PUBLICATION REVIEW

Publication of this technical documentary report does not constitute Air Force approval of the report's findings or conclusions. It is published only for the exchange and stimulation of ideas.

TABLE OF CONTENTS

LIST OF FIGURES

1. INTRODUCTION

This report represents the results of a one year research and development effort on a solar flat plate thermoelectric space power source. The major design criteria and objectives can be listed as follows:

(a) 300 mile orbit
(b) One year life (three years with thermal storage)
(c) 5-8 watts per square foot
(d) 15-20 watts/pound
(e) 50% of the values of (c) and (d) with thermal storage

The device consists of flat collector and radiator plates with thermoelements sandwiched between them. The collector plate must be coated with a spectrally selective optical coating having a high absorptivity in the visual portion of the solar spectrum and a low emissivity in the infra-red portion.

Earlier work in this area, utilizing lead telluride/zinc antimonide thermoelements resulted in a flight test that demonstrated the basic feasibility of the system (1, 2). Thermal analysis (3) indicated the possibility of achieving higher overall efficiency at lower operating temperatures because the properties of thermoelectric materials, generally, decrease as temperature increases and because radiation losses from the collector increase rapidly as temperature is increased. Based upon this analysis, bismuth telluride thermoelements at a hot junction temperature of 230°C were selected for this program.

The potential advantages promised by the solar flat plate thermoelectric generator are high reliability, light weight and low cost. The high reliability is promised by (a) insensitivity to Van Allen radiation, (b) low operating temperatures, (c) test results under thermal cycling and booster environmental testing and (d) redundancy obtained by series/parallel thermoelement circuitry. The light weight is due to the minimum weight components and efficient structural design used. Ease of fabrication and minimal material weight account for the expectation of low cost.

A number of technical problems required investigation during this program and are discussed in detail in the sections that follow. The fabrication and testing of prototype panels submitted to the Research and Technology Division is also discussed.

Manuscript released by Robert E. Rush, Author, September 14, 1964, for publication as an RTD Technical Documentary Report.

2. SYSTEM DESCRIPTION

The solar flat plate thermoelectric generator is shown, in its simplest form, in the sketch below.

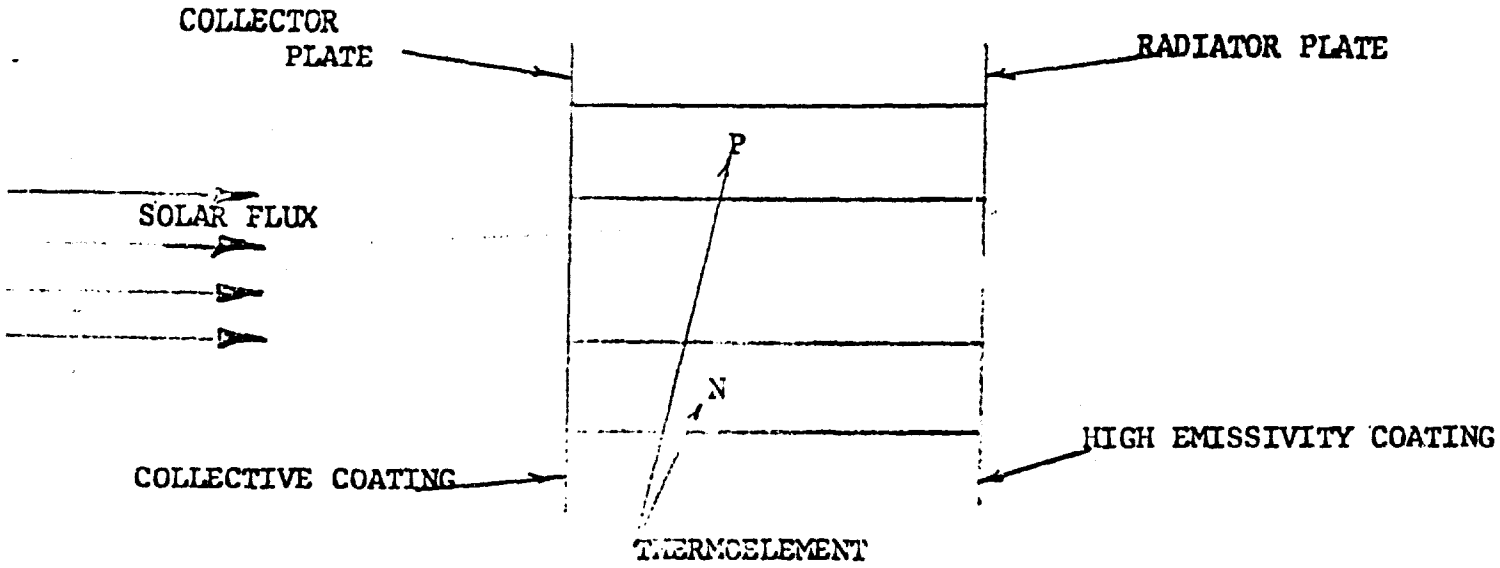

The collector plate, made of aluminum foil, is coated with a multilayer silicon monoxide/aluminum coating. This coating has a high absorptivity in the visual portion of the spectrum allowing efficient collection of the incident energy. The coating provides a low infra-red emissivity so that the heat lost from the collector by radiation is limited. The aluminum foil radiator is provided with a high emissivity coating for efficient heat rejection.

Thermoelectric elements are located between these two plates, the hot junction formed at the collector plate and the cold junction at the radiator plate. The elements are connected in a series/parallel arrangement for increased reliability. Except for that fraction of the heat which is radiated directly between the plates, all of the input energy, less the heat reflected or radiated by the collector, is available for conversion by these thermoelements. Thermal and electrical loss considerations dictate that the distance between thermoelements be small. Weight considerations dictate in turn that the elements be of a small size.

3. THERMAL & THERMOELECTRIC DESIGN

The sketch below illustrates the heat balance for a solar flat plate (SFP). The first step in system design is to find that set of collector and radiator temperatures (T_1 and T_2) which maximize the power output of the device.

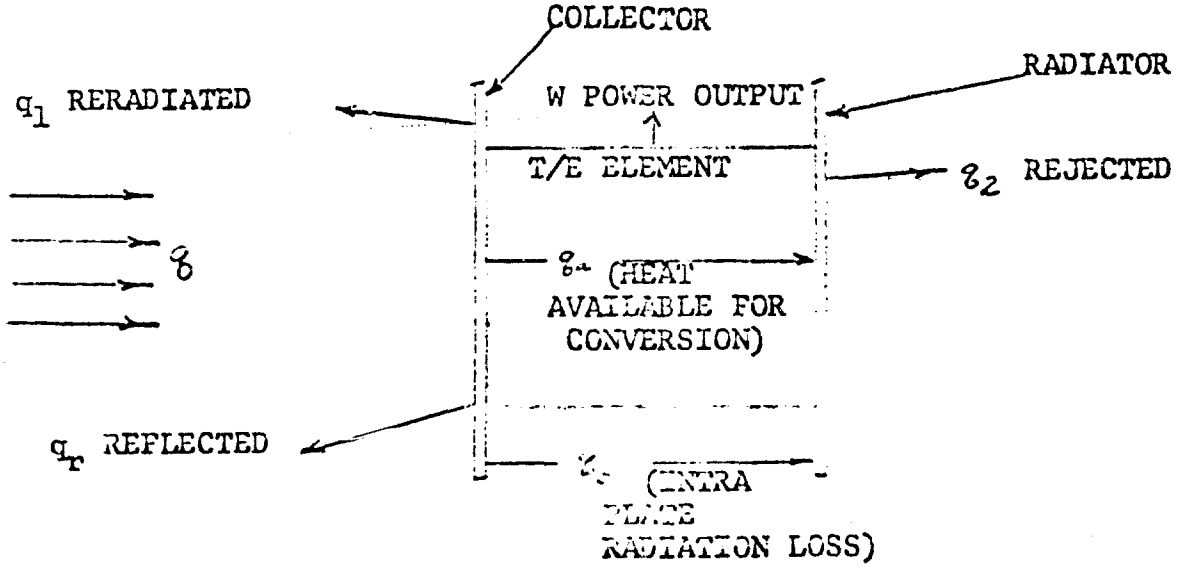

The following relationships are readily apparent*.

$$q - q_r = aq \quad (a = \text{collector absorptivity})$$

$$aq = q_1 + q_2 + w = q_3 + q_a + w + q_1$$

Since w is small it can be neglected.

$$aq = q_1 + q_2 = q_a + q_3 + q_1$$

$$q_a = q_2 - q_3$$

$$q_1 = \sigma E_1 T_1^4$$

*This discussion is based on a converter of unit area normal to the Sun.

$$q_2 = \sigma E_2 T_2^4$$

$$q_3 = \frac{E_3}{2-E_3} \sigma \left(T_1^4 - T_2^4 \right)$$

σ = Stefan Boltzman constant

E_1 = Emissivity of collector

E_2 = Emissivity of radiator

E_3 = Emissivity between plates

With these relationships it is possible, given a, E_1, E_2 and E_3, to select a collector temperature T_1, and to determine unique values of T_2 and q_a.

From (4) the following relationship can be obtained:

$$\eta_{T/E} = \frac{T_1 - T_2}{T_1} \cdot \frac{M-1}{M + \frac{T_2}{T_1}}$$

$$M = \sqrt{1 + \frac{Z}{2}(T_1 + T_2)}$$

$\eta_{T/E}$ = Thermoelectric Converter Efficiency

Z = Thermoelectric Figure of Merit (including contact resistances and temperature dependence)

$$w = \eta_{T/E} \cdot q_a$$

For each set of values of T_1, T_2, Z, and q_a there exists, therefore, a unique value of $\eta_{T/E}$ and w. The goal of this system design procedure is to maximize the value of w. The method used is to select successive values of T_1 and solve for w, finding a maximum. The values of a, E_1, E_2, E_3, and Z required for the solution are defined in Section 4 of this report.

The second step in system design is to determine the size and spacing of the thermoelements to be used in the device.

From (4) the following relationships can be obtained:

$$q_a = q_n + q_p$$

$$q_n = K \left(A_g / \ell\right) \quad (T_1 - T_2)$$

$$q_p = N \alpha I T_1$$

$$Vo = N \alpha (T_1 - T_2)$$

$$Vc = \frac{M}{M + 1} \quad (Vo)$$

$$w = Vc \ (I)$$

where: q_n = heat transferred through the thermoelements by conduction

q_p = heat transferred through the thermoelements by Peltier pumping

K = thermal conductivity of the thermoelements

A_g = total thermoelement cross section area

ℓ = thermoelement length

N = number of thermocouples

α = Seebeck coefficient of the thermocouples

I = current, amperes

Vo = open circuit voltage

Vc = closed circuit voltage

Given q_a, K, T_1, T_2, N, α, Z, and w, it is possible to determine A_g/ℓ. In Section 4.2 it will be shown that a suitably sized thermoelement is .080" x .080" x .100" long.

Since ℓ and A_g/ℓ are now both defined it is obvious that A_g is now known. The number of thermoelements, Ne, per square foot, is, therefore, $A_g/(.08" \times .08")$. Once Ne is known the spacing between elements is also known.

4. COMPONENT & PROCESS DEVELOPMENT

4.1 Optical Coating

One of the most critical areas in this development effort is the spectrally selective collector coatings. Early in the program, a number of possible industrial sources for such coatings were contacted for evaluation samples. The only source from which samples were actually obtained was Kinney Vacuum Company, Camden, New Jersey. These samples were submitted to the Air Force and measurements* were made, using a solar simulator, of absorptivity and reflectivity as a function of temperature. The results are given in Figure 4-1. This data is of obvious value in the design of a solar thermoelectric converter. Based on these results Kinney was selected to apply the coating to the collector plates of the prototype converters fabricated during this program.

4.2 Thermoelectric Materials

Certain criteria have been established as a guide to thermoelectric material selection for solar flat plate thermoelectric generators:

(a) Figure of Merit, Z, as a function of temperature.
(b) Availability and structural qualities in small size.
(c) Life (integrity and stability) in a thermal cycling and vacuum environment.
(d) Availability of contacting techniques having a low junction resistance and appropriate life characteristics.

In a previous study (3) it was shown that the bismuth telluride alloys are the thermoelectric materials of choice for the SFP application in an Earth orbit. This is so because the bismuth telluride materials have the highest figure of merit in the operating temperature range that is most suitable for existing collector coatings.

The Figure of Merit, Z, for various types of bismuth telluride has been determined as a function of temperature. This determination was made experimentally, using the well known "ΔT max." technique (4). This technique consists of operating assembled thermocouples in the cooling mode and searching for that value of current which causes the largest temperature difference across the thermocouple. Ideally, there should be zero heat input or output at the cold junction. The temperature measurements can be related as follows:

$$(T_h - T_c)_{\text{maximum}} = 1/2\ Z\ T_c^2$$

*The measurements were made at the Naval Radiological Defense Laboratory, Hunters Point, Calif.

T_h = hot junction temperature, °K

T_c = cold junction temperature, °K

Z = Figure of Merit, $°K^{-1}$

Several types of thermoelements were tested and the .080" x .080" x .100" elements manufactured by Melcor, Inc., were found to be most suitable for this application. Figure 4-2 presents the results of the tests of these elements. Also presented for comparison are the test results of large size Melcor elements. One important point, immediately evident from this data, is that when elements are processed to the small sizes required for this application, they suffer a reduction in the Figure of Merit of approximately 16% at operating temperatures. This reduction is far more than would be expected from contact resistance alone. One possible explanation is that microcracks develop during the cutting operation.

4.3 Structural Support

Panel support structure has been defined as any feature or component included in panel design for handling ease or vibration and shock resistance. A number of design concepts have been considered and several have been tested.

One 4" x 4" panel, designated F-1, was constructed as shown in Figure 4-3. This panel used a plastic foam, Emerson and Cumming Eccofoam SH at 8 pounds per cubic foot density, cemented to the radiator plate for support. An aluminum reflector sheet was also cemented to the foam. Holes were drilled through the foam and the reflector sheet to allow passage of the thermoelements. This panel was then thermally cycled in a vacuum of about 10 microns. The collector temperature was cycled between 450°F and 100°F while the radiator temperature varied between 260°F and 75°F. After a few cycles, severe warping of the radiator structure was observed. This was probably due to the fact that the plastic foam and the aluminum had different coefficients of expansion. No further work on foam support structures was performed.

A 4" x 4" panel, designed H-1, was built using a radiator support structure of aluminum honeycomb weighing 4.3 pounds per cubic foot. (Hexcell Corp. 1/4" cell size, 0.002" aluminum). This honeycomb was cemented to the radiator plate using mylar sheet as electrical insulation. An aluminum foil reflector sheet was also used. The construction is shown in Figure 4.4. This support structure did not warp under thermal cycling. Warping of the collector plates was observed, however.

In the F-1 panel, stress-relief slots were used on two of the four collector sheets similar to those described in (1). On the H-1 panel, these slots were extended across the entire strip. In all cases severe warping of the collectors under thermal cycling was observed. This warping caused extensive thermoelement failure.

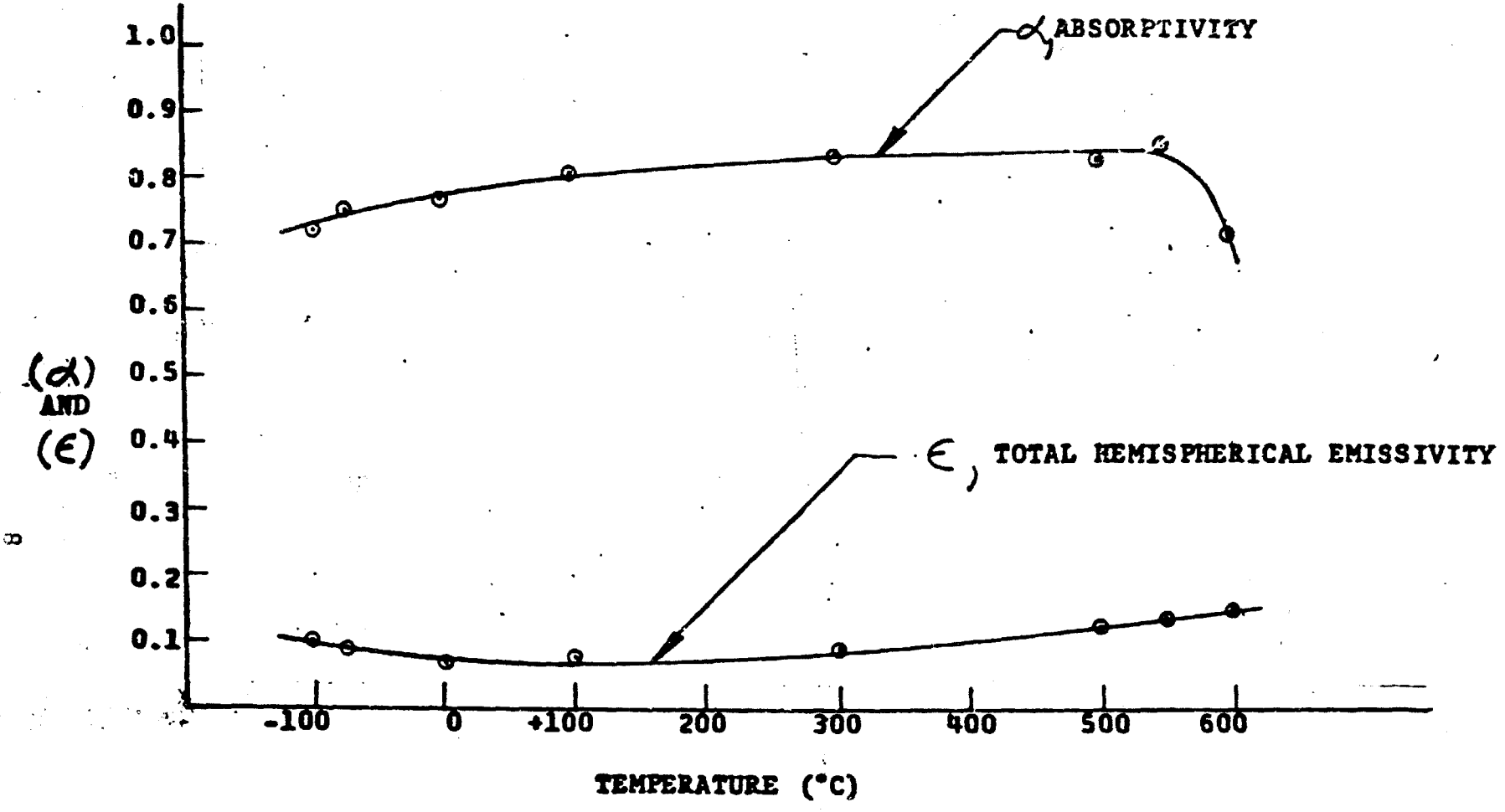

ABSORPTANCE AND EMITTANCE VERSUS TEMPERATURE FOR SPECIMEN ASD-208- (KINNEY VACUUM COMPANY)

FIGURE 4-1

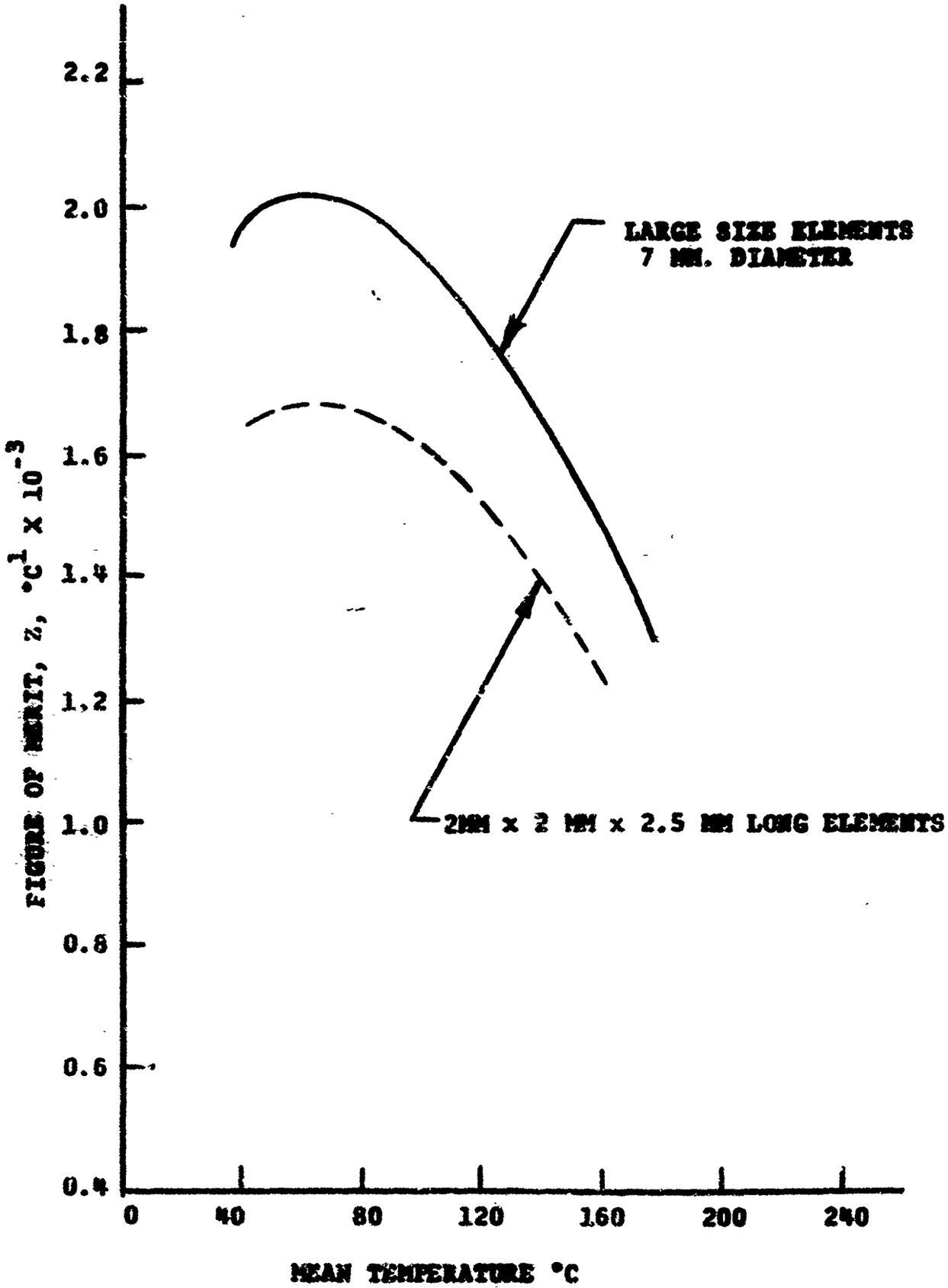

FIGURE 4-2

FIGURE OF MERIT VS. TEMPERATURE FOR BISMUTH TELLURIDE THERMOCOUPLES OF VARIOUS MATERIAL

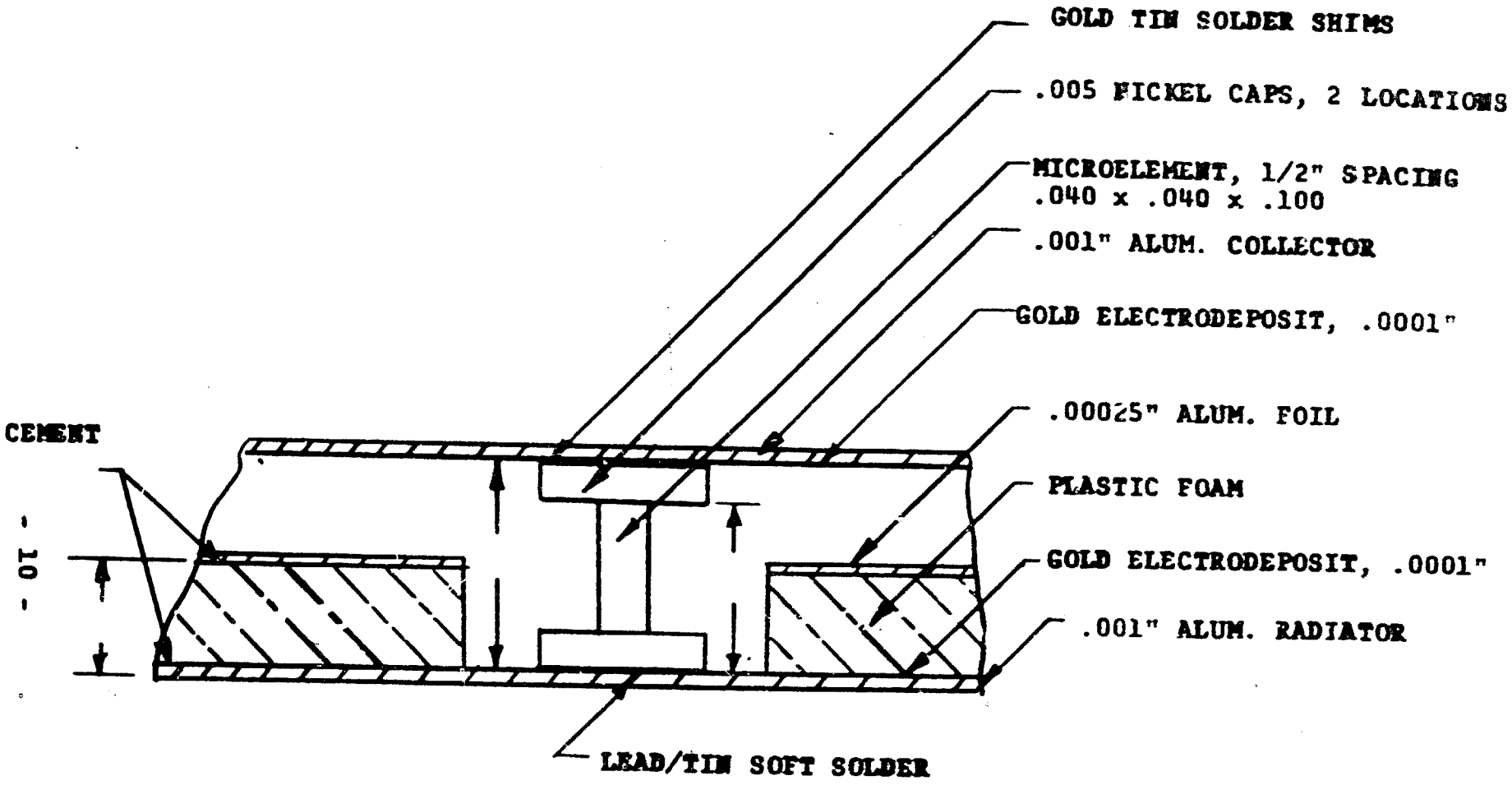

FIGURE 4-3

CROSS SECTION VIEW OF SOLAR FLAT PLATE
CONVERTOR WITH PLASTIC FOAM
SUPPORT STRUCTURE

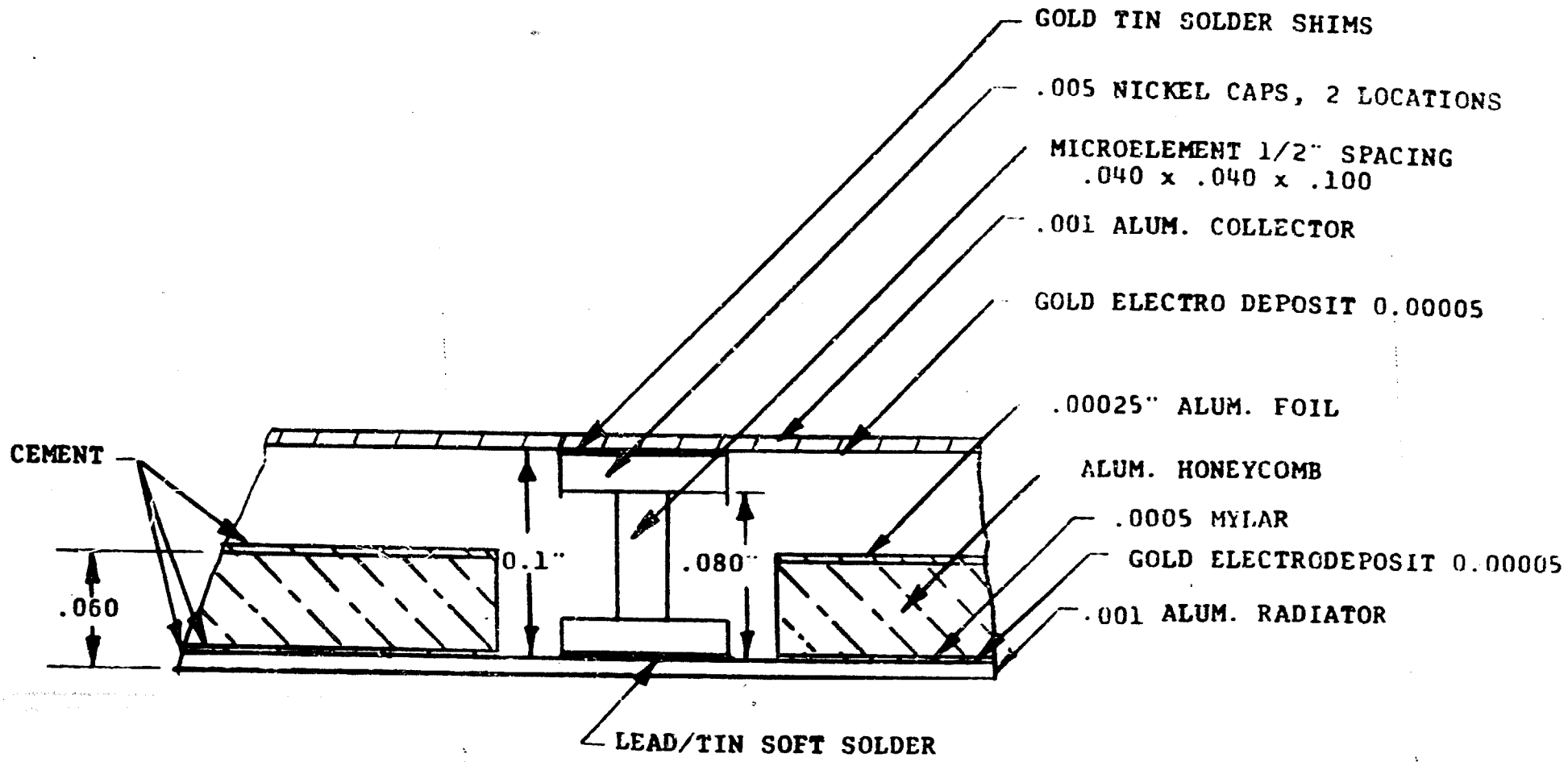

FIGURE 4-4

CROSS SECTION VIEW OF SOLAR FLAT PLATE CONVERTOR WITH ALUMINUM HONEYCOMB SUPPORT STRUCTURE.

Consideration was then given to two other structural design concepts. One of these, the so-called "bowed" design is shown in Figure 4.5. After intensive study, it was decided that this approach presented formidable fabrication problems. The other concept, designated "integral reinforced plate" or IRP is shown in Figure 4.6. Structural value is provided by folding plate members into open boxes and by thin walled aluminum tubular members. Table 4-1 compares, in a qualitative manner, the various structural concepts considered.

Study of Table 4-1 indicated that the IRP concept merited further investigation. A number of panels were subjected to thermal cycling without structural failure. These tests are described further in Section 5.2.

A program of sinusoidal vibration testing was then conducted according to the following schedule:

Frequency Range		Displacement	Loading
Lower Limit	Upper Limit	(Double Amplitude)	
5 cps	14 cps	0.5"	-
14	40	-	5 g
40	400	-	7.5 g
400	3000	-	15 g

A single sweep was carried out at a constant octave rate in a minimum interval of 45 minutes from the lower to the higher frequency limit. The panels were tested in three axes. Table 4-2 gives a description of the panels tested and the test results. Because of the promising results and low weight, the IRP design was developed to the point where panels could withstand the vibratory environment. A complete description of the final design is given in Section 6.

4.4 Joining and Bonding Procedure

The term "joining" is defined as the contacting of the semiconductor thermoelement to a metallic conductor. The term "bonding" is defined as the contacting of the above mentioned metallic conductor to the radiator and collector sheets. Accelerated thermal cycling tests were used as the primary method of evaluating joining and bonding techniques.

The earliest panels built under this program used contacts as shown in Figure 4.7. An electrodeposited layer of gold was applied to the aluminum foil so that the thermoelement assemblies could be attached, by soldering, to the foil. A number of problem areas with this procedure were uncovered when panel B-4 was exposed to thermal cycling. (See Section 5.2 for test results)

1. Severe corrosion of the collector plate was observed at the end of the test. This was diagnosed as the formation of a gold/aluminum intermetallic compound ($Al\ Au_2$).

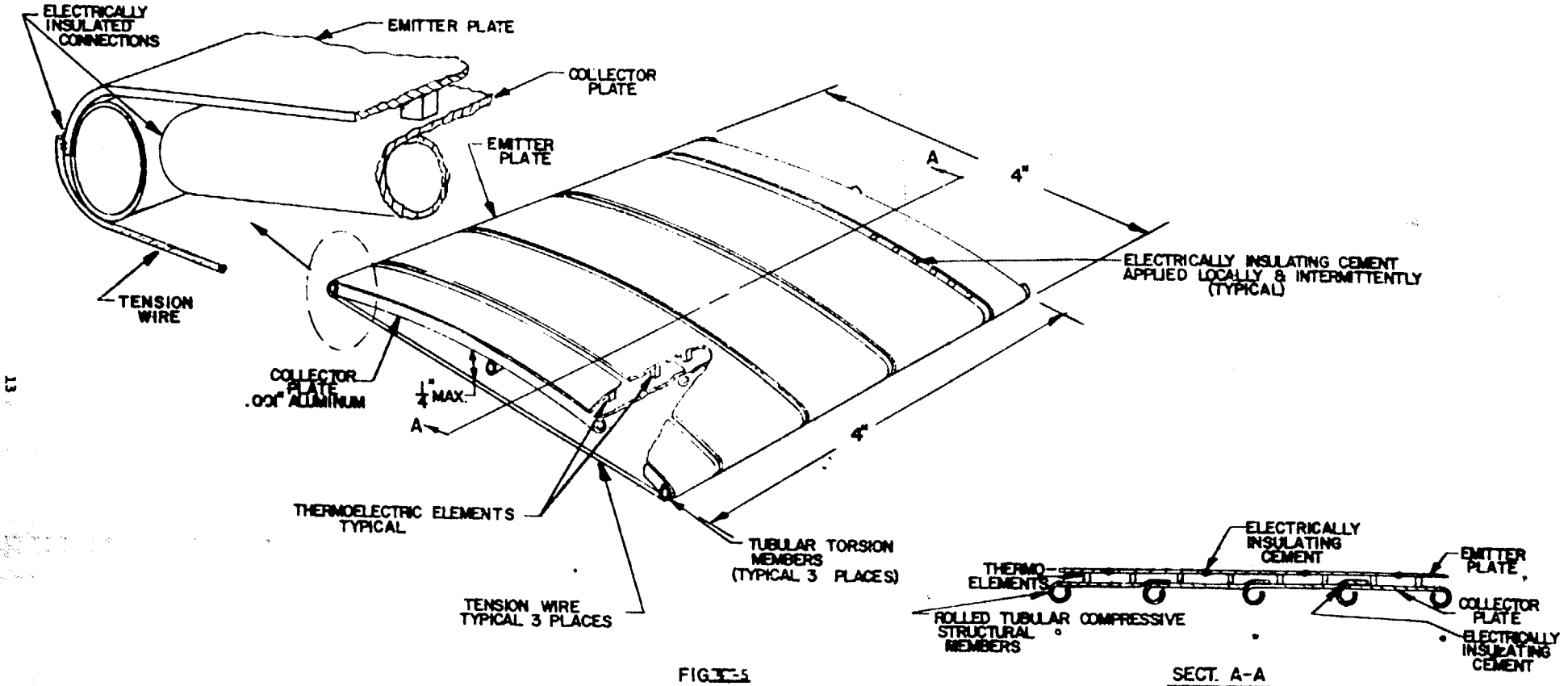

FIG. 5

RIGID DESIGN-SOLAR FLAT PLATE

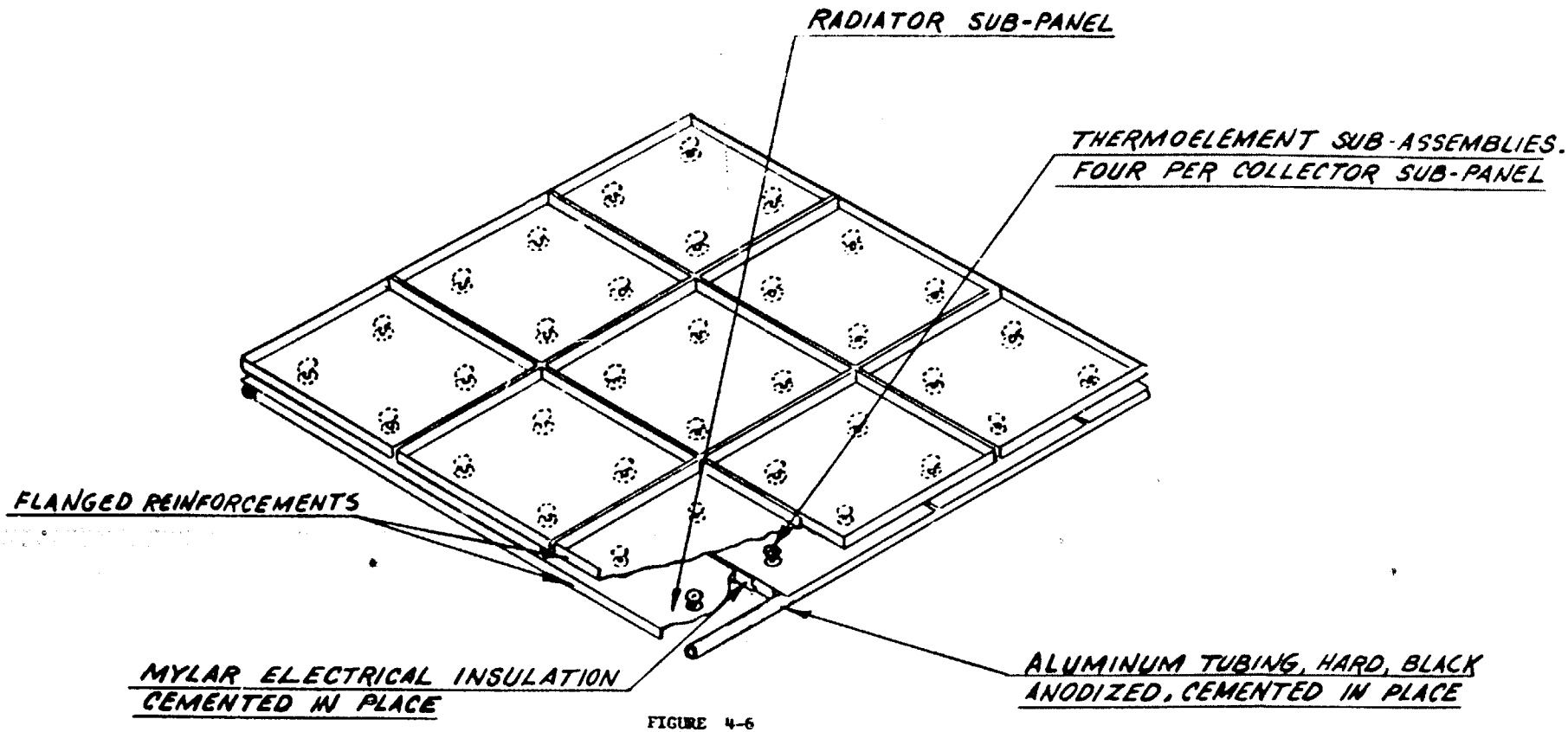

FIGURE 4-6

IRP DESIGN - SOLAR FLAT PLATE

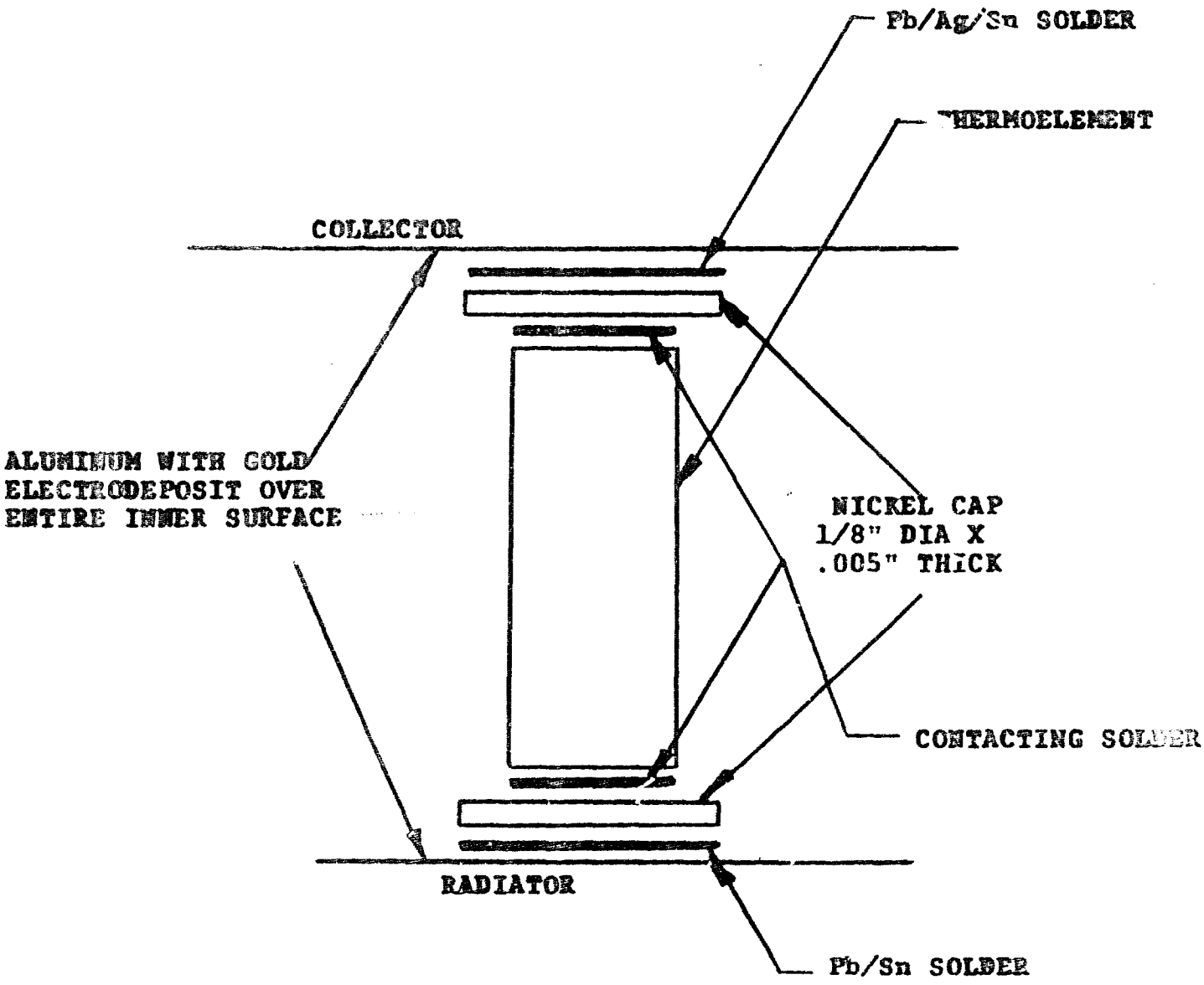

FIGURE 4-7

JOINING AND BONDING PROCEDURE - INITIAL

TABLE 4-1

Comparison of Support Structure Designs

Property	Honeycomb	Bowed	Integral Reinforced Plate (IRP) (BOX)
Weight (All three concepts have approximately equal weights)	Radiator support structure weighs approximately 14 grams/square ft.	Required structural component requirements are such that a weight equal to that of the "integral reinforced plate" structure is estimated	Radiator support structure weighs 14 grams/square foot maximum
Electrical insulation integrity	Most difficult because of necessity of insulating honeycomb from radiator plate	More difficult than the "IRP" because of members that go between the radiator and the collector	Very easy to insulate.
Collector thermal expansion	Not a problem if small collector sub-plates are used	A possible problem area because collector cannot be divided into sub-plates	Not a problem if small collector sub-plates are used
Potential loss due to a quality control reject of one collector bond	Maximum loss is one sub-panel of four thermoelements	Maximum loss is one sub-panel of 12-16 thermoelements, depending upon collector spacing	Maximum loss is one sub-panel of four thermoelements
Ease of fabrication	Some problems due to requirement of electrical insulation and handling of honeycomb	Expected most difficult	Fabrication is extremely simple

TABLE 4-2. VIBRATION TESTING, SUPPORT STRUCTURE DEVELOPMENT

Test No.	Sample No.	Sample Description	Test Description	Test Results	Comments
1	B-5	IRP, .001" aluminum (1100-0) collector and radiator plates, 4.8" x 4.8" area, 36 thermo-elements (0.08" x 0.08" x 0.10" long) on 0.8" centers. Aluminum tubular (.002" wall, hardcoated) framing around radiator plate periphery. Gold plating on radiator and collector sheets.	Tested in horizontal plane only.	Failures occurred at 400 cps. Thermoelements broke through collector in two locations. Two other elements broke through both collector and radiator.	The test mounting fixture found to be inadequate.
2	B-20	Identical to B-5 except gold plating replaced by selective nickel plating 1/4" diameter x .001" thick.	(a) Tested in two axes. (b) Tested from 5-9 cps in horizontal plane. (c) Tested from 3000-13 cps in horizontal plane.	(a) No failures in vertical axes. (b) At 9 cps 0.5" double amplitude one collector panel with four elements attached separated from collector plate. (c) Omitted, see original manuscript.	Re-designed test mounting fixture used and found to be satisfactory.
3	B-29	IRP, 4" x 4" size, collector and radiator panels of .001" thick aluminum (1145), .08" x .08" x .10" long thermo-elements on 1.0" centers. Aluminum tubular framing as in B-5 plus an additional aluminum tube in center of radiator panel.	The entire vibration spectrum was applied.	No failures occurred.	

TABLE 4-2 (Con't.)

Test No.	Sample No.	Sample Description	Test Description	Test Results	Comments
4	B-30	Same as B-29 except radiator plate was made of .0015" aluminum foil (5050-H38).	The entire vibration spectrum was applied.	No failures occurred.	
5	B-31	Same as B-29 except .002" thick aluminum used for the radiator.	The entire vibration spectrum was applied.	No failures occurred.	
6	B-32	IRP, 4.8" x 4.8" size, .08" x .08" x 0.10" long thermoelements on 0.8" spacing, collector of .001" thick aluminum foil (1145), radiator of .0015" thick aluminum foil (5050-H38) center tube as in B-29.	The entire vibration spectrum was applied.	No failures occurred.	

2. Solder bonds, both collector and radiator, were open on a large number of samples. This was diagnosed as alloying of the lead/tin bonding solder with the joining solder resulting in a low melting point alloy.

Problem (1) was resolved by substituting nickel for the gold electrodeposit. Because a thicker layer of nickel than of gold is required for soldering, weight considerations dictated that the nickel be applied only where needed for thermoelement contacts. The nickel was, therefore, electrodeposited in a selective manner.

Problem (2) was resolved on the collector side by eliminating the nickel cap of Figure 4-7 and soldering the thermoelement directly to the electrodeposited nickel. A nickel cup, 1/4" diameter by 0.002" thick, was used on the radiator side to prevent solder cross-over. The resultant contacting methods are shown in Figure 4.8. A discussion of the experimental evaluation of this procedure will be found in Section 5. All delivery prototype panels used these joining and bonding techniques.

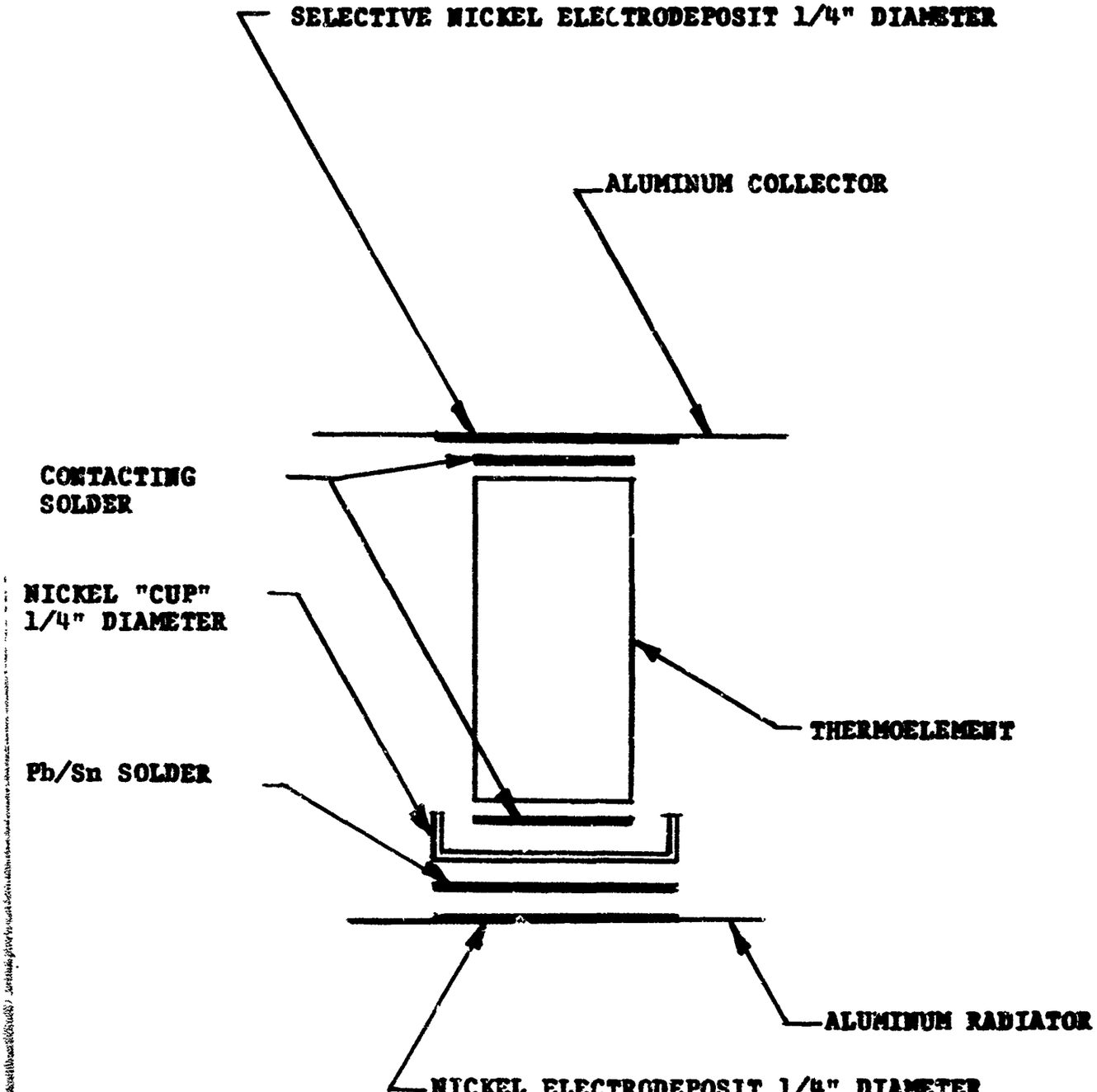

FIGURE 4-8

JOINING AND BONDING PROCEDURE - FINAL

5. DEVELOPMENTAL TESTING

5.1 Resistance Stability

In accordance with contractual requirements, a test was performed to determine resistance changes of thermoelement assemblies as a function of time at constant temperature. Six positive thermoelements and six negative thermoelements were tested. The element size was 2mm x 2mm x 2.5mm long. Figure 5.1 shows the sample construction while Figure 5-2 shows the test apparatus arrangement. The cold junctions of all the elements were water cooled while the hot junctions were heated with infrared lamps.

The test was run for a total duration of 1,000 hours. Frequent readings of thermoelement resistance and temperature were taken. The test results are plotted on Figures 5-3, 5-4, and 5-5. Both resistance and hot junction temperature data are presented.

Examination of the data has led to the following observations:

1. Day to day fluctuations were present in the resistance readings. These fluctuations were as much as $\pm$ 10%. The variation in hot junction temperature is believed to have caused a part of this resistance variation. Reading errors, may, of course, be the cause of some of the more severe day to day changes. The changes where resistance is seen to decrease are believed to be caused by improvement of the element junctions occuring with time and temperature in vacuum. Conversely, some of the resistance increases may have been caused by local junction separation caused by thermal stresses.

2. In spite of the day to day variations in individual elements, the average resistance of all samples was remarkably stable. For example, the total resistance of all 12 elements increased by only 1.0% during the 1,000 hours. Considering the fact that the temperatures were slightly higher at the end of the test than at the start, the true change in sample resistance, which is a function of temperature, was actually less than 1%.

3. One of the difficulties that developed in this test was non-uniform hot junction temperatures. This temperature spread can be seen in the data of Figures 5-3, 5-4 and 5-5.

4. Readings were not taken after 550 hours for samples PB and NB because of failures in the wires used for measurements.

5.2 Thermal Cycling

As mentioned above, the primary method adopted for evaluating bonding and joining procedures during the development program was accelerated thermal cycling in vacuo. This was considered to be an efficient method of uncovering defects in techniques or materials. Because the solar flat plate thermoelectric generator is a very simple device, a number of design changes can be incorporated into one sample without one phenomena masking another.

FIG. (5-1)

ELEMENT SUB-ASSEMBLY FOR SUBLIMATION TEST

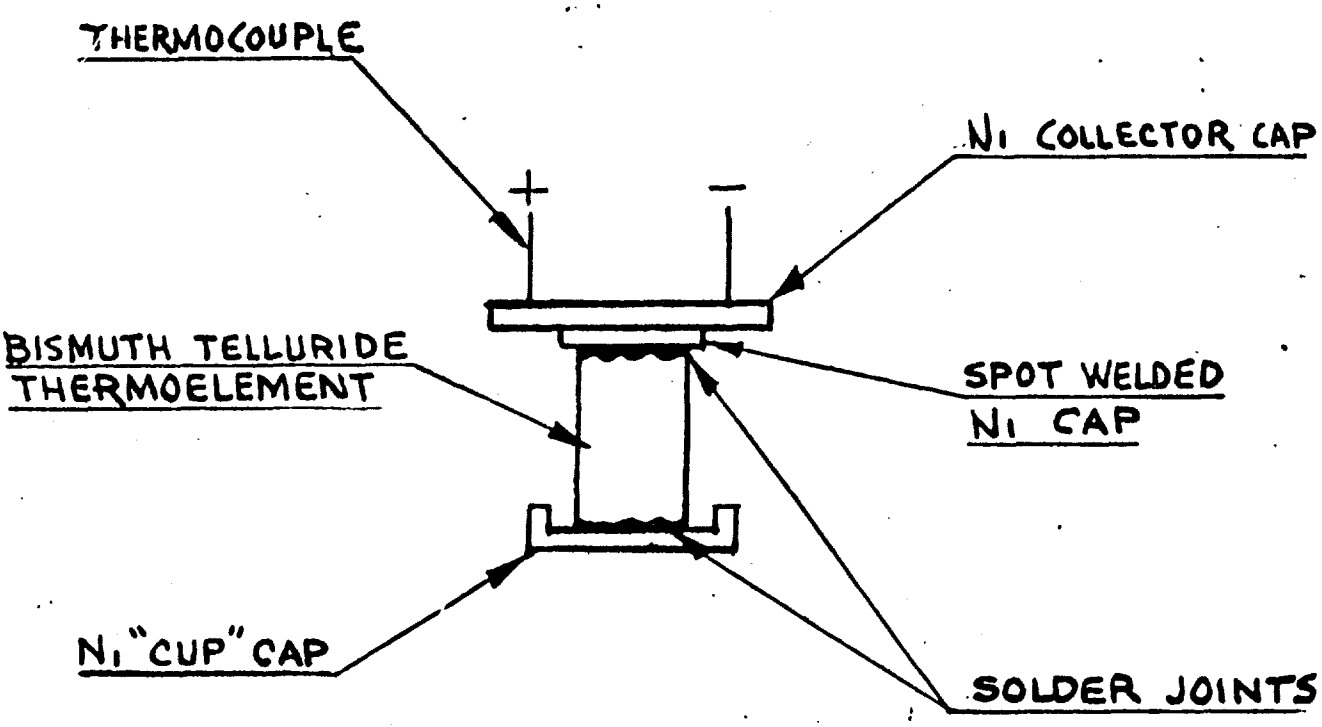

FIG. (5-2)

SUBLIMATION TEST RIG ASSEMBLY

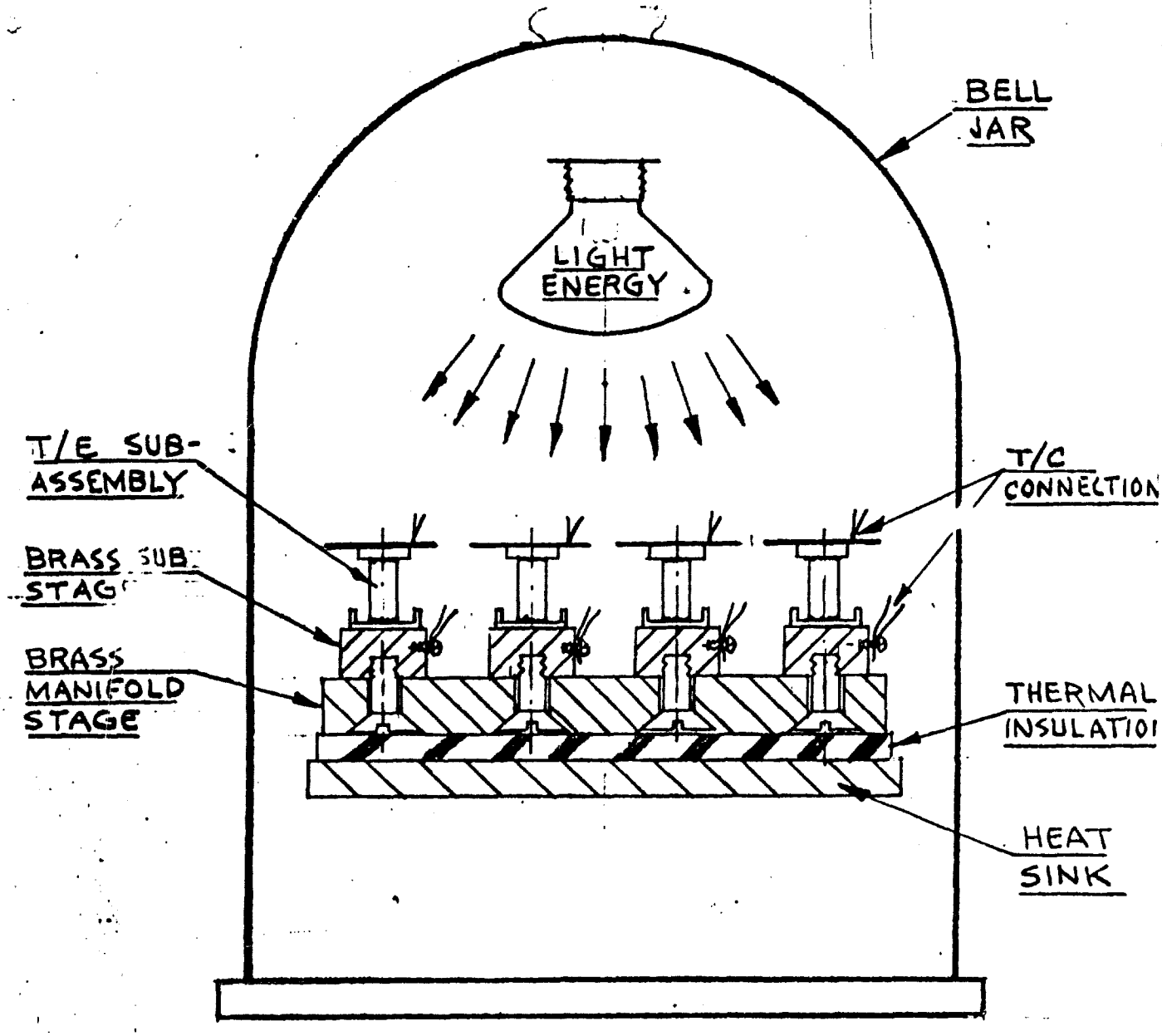

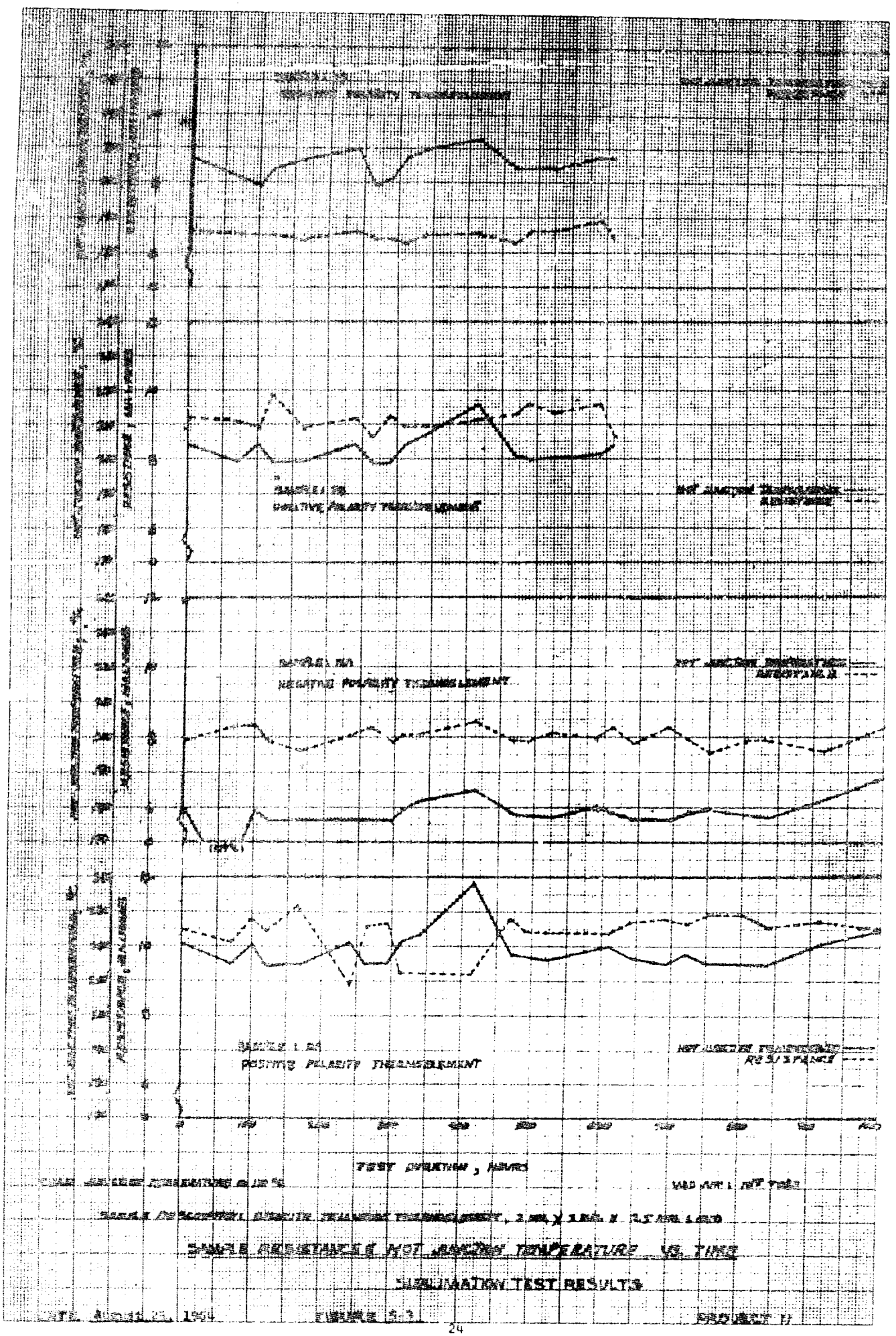

SAMPLE RESISTANCE & HOT JUNCTION TEMPERATURE VS. TIME

SUBLIMATION TEST RESULTS

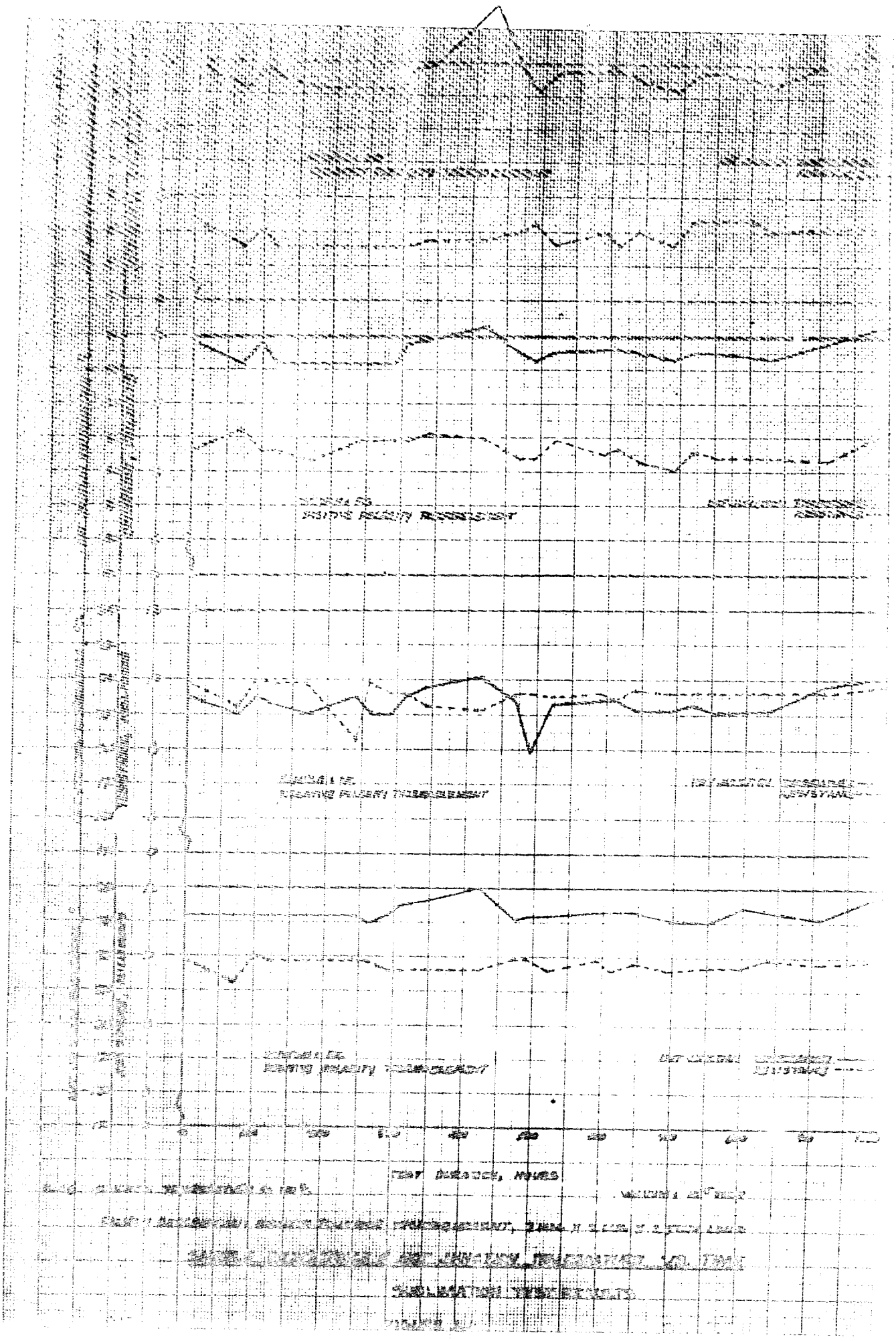

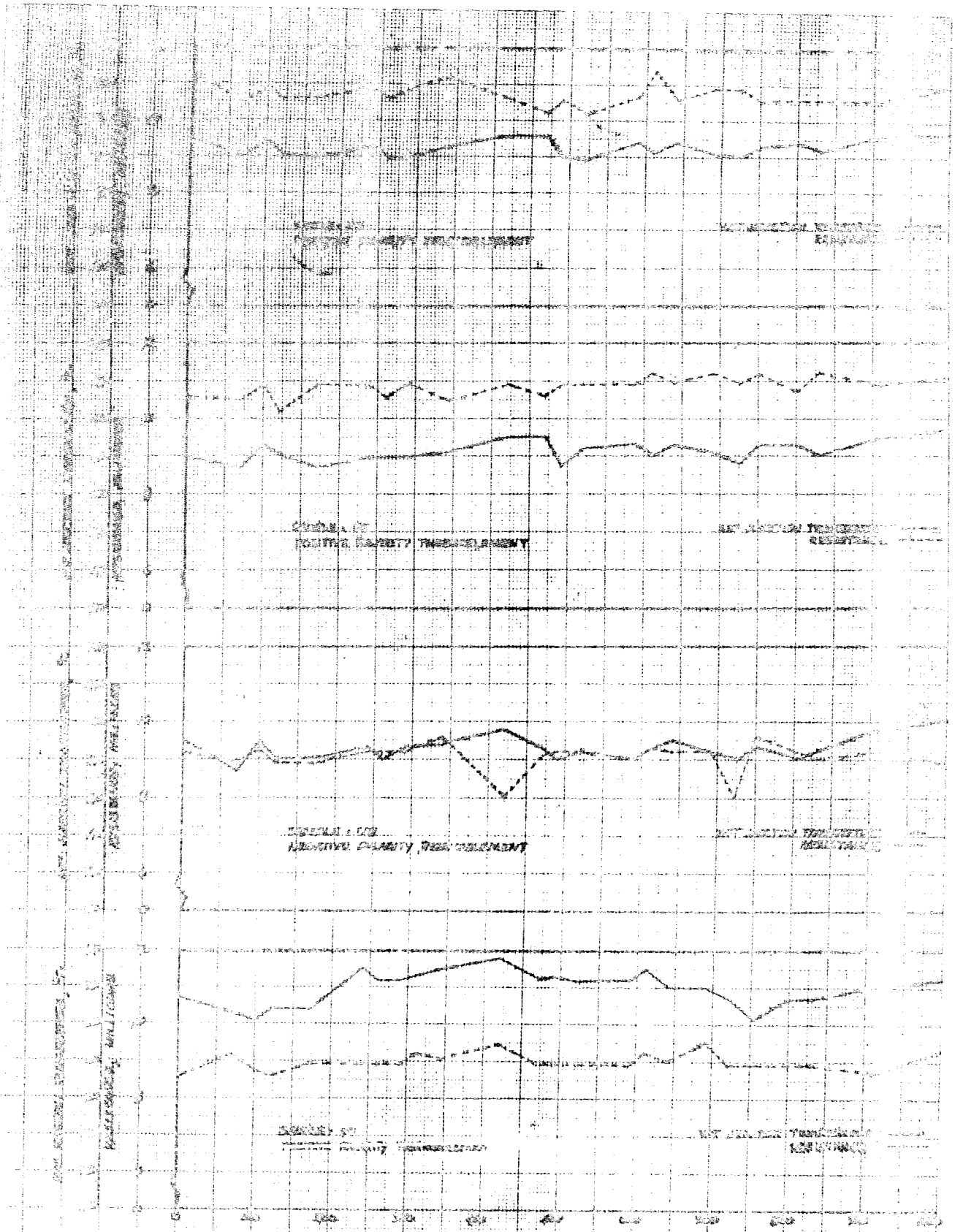

Table 5-3 presents a sample description, test method and summary of results for the various samples tested. Tables 5-4 and 5-5 give bonding procedures for various samples. Figures 5-6 and 5-7 give test data for certain samples.

The purposes of the various thermal cycling tests were for evaluation of structural designs, thermoelement processing or bonding techniques. The purpose and results of specific tests are discussed in Section 4 of this report.

TABLE 5-3. THERMAL CYCLING TEST DATA

Test No.	Sample No.	Panel Description	Purpose of Test	Test Conditions	Total No. of Cycles	Test Results	Comments
1	F-1	Plastic foam support structure, See Figure 4.3.	Evaluation of foam support structure concept.	10^{-2} Torr, Cycle: 1/2 hr., on, 1/2 hr. off T_{hot} cycled 232°C to 38°C. T_{cold} cycled 127°C to 21°C	20	Severe warping of radiator, support structure and collector. Failure of several thermoelements, evidence of oxidation and excessive temperature.	Support structure warping due to differential thermal expansion. Vacuum and temperature distribution require improvement.
2	H-1	Honeycomb support structure, See Figure 4.4 (Hexcell Corp. Honeycomb, 1/4" cell size, 0.002" aluminum foil).	Evaluation of honeycomb support structure	Same as F-1	20	Collector panel warping, thermoelement failures, evidence of oxidation and excessive temperature.	
3	B-1	Integral reinforced plate (IRP) structure (no tubular support members) 1" x 1" square collector, 4" x 4" size 32 P and 32 N thermoelements on 0.5" spacing. See Figure 4.6 for general configuration.	Evaluation of IRP concept	10^{-3} Torr, Cycle 1/2 hr. on, 1/2 hr. off. T_{hot} cycled 230°C to 40°C. T_{cold} cycled 130°C to 20°C. Test apparatus flushed with 85% N_2/15% H_2 during every cooling cycle.	18	Evidence of thermoelement failure due to oxidation, structure appeared to need additional support.	Probability that element oxidation occurred during fabrication.

TABLE 5-3 (Con't.)

Test No.	Sample No.	Panel Description	Purpose of Test	Test Conditions	Total No. of Cycles	Test Results	Comments
4	F-2	Plastic foam support structure on radiator with 1" x 1" IRP type collector, 1" x 4" size.	Re-test of foam support structure.	Same as B-1 except T_{hot} cycled 210°C to 40°C	58	Severe radiator warping, thermoelement failure believed due to oxidation.	Same as B-1
5	B-2	IRP structure similar to B-1 except 1" x 4" size.	Evaluation of effect of change in thermoelement processing.	Same as F-2	58	Very little evidence of oxidation. Process problem still present because of many thermoelement failures.	
6	B-3	IRP structure, 1.6" x 1.6", collectors, 4 thermoelements, 0.08" x 0.08" x .10" long.	Evaluation of larger size thermoelements.	5×10^{-6} Torr., cycled: 6 min. on/6 min. off T_h 230°C-40°C T_c 150°C-20°C	117	All bonds were satisfactory. One failed thermoelement contact.	
7	B-4	IRP structure, 1.6" x 1.6" collectors, 4.8" x 4.8" panel, 36 thermoelements, 0.08" x 0.08" x .10" long.	To evaluate improved controls on thermoelement processing.	Same as B-6	2000	See Figure 5.6 for resistance vs. cycle data. See Section 7 for bonding problem discussion.	

TABLE 5-3 (Con't.)

Test No.	Sample No.	Panel Description	Purpose of Test	Test Conditions	Total No. of Cycles	Test Results	Comments
8*	B-16	1.6" x 1.6" square panel, 2 negative and 2 positive polarity thermoelements on 0.8" spacing. 0.08" x 0.08" x .10" long thermoelements.	Evaluation of: Collector bonding technique A* Radiator bonding technique B*	See Figure 5-7	5500	See Figure 5-7 for resistance vs. cycle data. See Section 4.4 for bonding problem discussion.	
9	B-17	Same as B-16	Same as B-16	See Figure 5-7	7000	See Figure 5-7	
10	B-18	Same as B-16	Evaluation of: Collector bonding technique C Radiator bonding technique B	See Figure 5-7	5500	See Figure 5-7	
11	B-19	Same as B-16	Same as B-18	See Figure 5-7	5200	See Figure 5-7	
12	B-21	Same as B-16	Evaluation of: Collector bonding technique C Radiator bonding technique D	See Figure 5-7	1600	See Figure 5-7	
13	B-22	Same as B-16	Same as B-16	See Figure 5-7	3600	See Figure 5-7	
14	B-23	Same as B-16	Evaluation of: Collector bonding technique D Radiator bonding technique D	See Figure 5-7	3600	See Figure 5-7	

*For test numbers 8 through 28 see Tables 5-4 and 5-5 for description of collector and radiator bonding techniques.

TABLE 5-3 (Con't.)

Test No.	Sample No.	Panel Description	Purpose of Test	Test Conditions	Total No. of Cycles	Test Results	Comments
15	B-26	Same as B-16	Evaluation of: Collector bonding technique G Radiator bonding technique B	See Figure 5-7	3600	See Figure 5-7	
16	B-27	Same as B-16	Evaluation of: Collector bonding technique E Radiator bonding technique B	See Figure 5-7	4600	See Figure 5-7	
17	B-28	Same as B-16	Same as B-27	See Figure 5-7	4600	See Figure 5-7	
18	B-33 B-34 B-35	Same as B-16	Evaluation of: Collector bonding technique E Radiator bonding technique F	3×10^{-5} Torr., Cycle: 6 min. on/6 min. off T_{hot}, 240°C to 40°C. T_{cold} 130°C to 20°C.	800	No change in panel resistance.	

TABLE 5-4

Description of Bonding Techniques Evaluated For Both Collector and Radiator

Type	Application	Description
A	Collector	1/4" diameter nickel cups soldered to thermoelements. Cups soldered to nickel plated aluminum collector with Pb/Ag/Sn solder.
B	Radiator	Same as A except use of Pb/Sn solder between cup and nickel plated aluminum radiator.
C	Collector	The thermoelements are soldered to 1/8" x 1/8" x 0.005" thick nickel straps. Straps spot welded to aluminum collector.
D	Collector or Radiator	Elements soldered to 1/8" diameter nickel caps, 0.002" thick. The cap is soldered to nickel plated aluminum with a solder that is compatible with the solder used for thermoelement to nickel contacting.
E	Collector	Thermoelement is soldered directly to a 1/4" diameter x 0.002" thick nickel disc spot welded to aluminum collector.
F	Radiator	1/4" diameter nickel cups soldered to thermoelements. Cups soldered with Pb/Sn solder to 1/4" diameter nickel disc spot welded to aluminum radiator.
G	Collector	1/4" diameter nickel cups soldered to thermoelements. Cups soldered with Pb/Ag/Sn solder to 1/4" diameter nickel disc spot welded to aluminum radiator.

TABLE 5-5

Tabulation of Bonding Techniques Used on Test Samples

Sample Number	Collector Bonding Technique	Radiator Bonding Technique
B-16	A	B
B-17	A	B
B-18	C	B
B-19	C	B
B-21	C	D
B-22	C	B
B-23	D	D
B-26	G	B
B-27	E	B
B-28	E	B
B-33	E	F
B-34	F	F
B-35	E	F

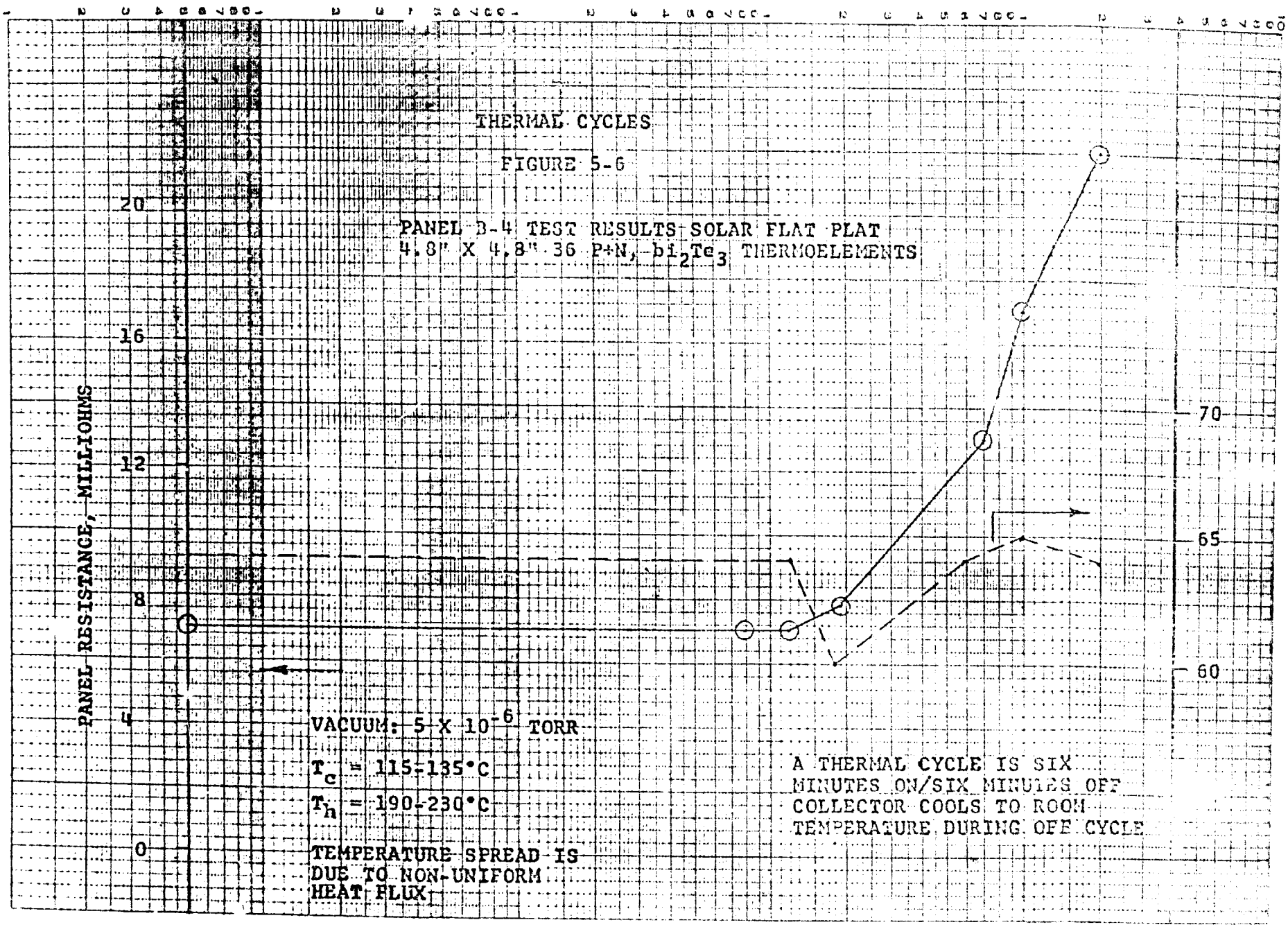

THERMAL CYCLES

FIGURE 5-6

PANEL B-4 TEST RESULTS SOLAR FLAT PLAT
4.8" X 4.8" 36 P+N, bi_2Te_3 THERMOELEMENTS

FIGURE 5-7. THERMAL CYCLING TEST RESULTS

6. PROTOTYPE PANEL FABRICATION

The final design of panels under this program was based upon the following:

(a) Thermoelement type and size was based upon the analysis described in Section 4.2.

(b) Thermoelement spacing was based upon the analysis of Section 3.

(c) The collector coating was based upon the work described in Section 4.

(d) The panel structural design was based upon the work described in Section 4.3.

(e) The joining and bonding procedures were based upon the work described in Section 4.4.

The 4" x 4" panel is depicted in Figure 6-1. This panel has two thermocouples in series with each leg of each thermocouple consisting of four thermoelements in parallel. Power leads and voltage measurement leads are supplied. Suitable temperature sensors are provided. The radiator is coated with "Krylon" flat black enamel. Figure 6-2 depicts a similar, 12" x 12", panel.

The fabrication procedure is as follows:

1. The radiator and collector plates are selectively electroplated with nickel.

2. Solder is applied to the electroplated areas.

3. The collector plates are coated by Kinney Vacuum Company, Camden, New Jersey, with spectrally selective coating.

4. The collectors are cut to size and folded.

5. The thermoelements (previously cut to size) are soldered to the nickel "cups".

6. The thermoelements are soldered to collectors, two positive elements and two negative elements on each collector sub-plate.

7. The radiator sub-panel is assembled with tubing, electrical insulation and cement as required.

8. The final assembly of collector sub-panels to radiator panel is then made.

Figure 6-3 is a photograph of a completed panel.

PARTS LIST

ITEM	DESCRIPTION	QTY
1	COLLECTOR	4
2	RADIATOR END	2
3	RADIATOR CENTER	1
4	T/E ELEMENTS-P&N	8 EA
5	Ni CUP	16
6	INSULATOR STRIP	2
7	Ni ELECTROPLATE	32
8	TUBULAR FRAME	1
9	Pb-Sn SOLDER	A/R
10	SOLDER	A/R
11	BONDING AGENT	A/R

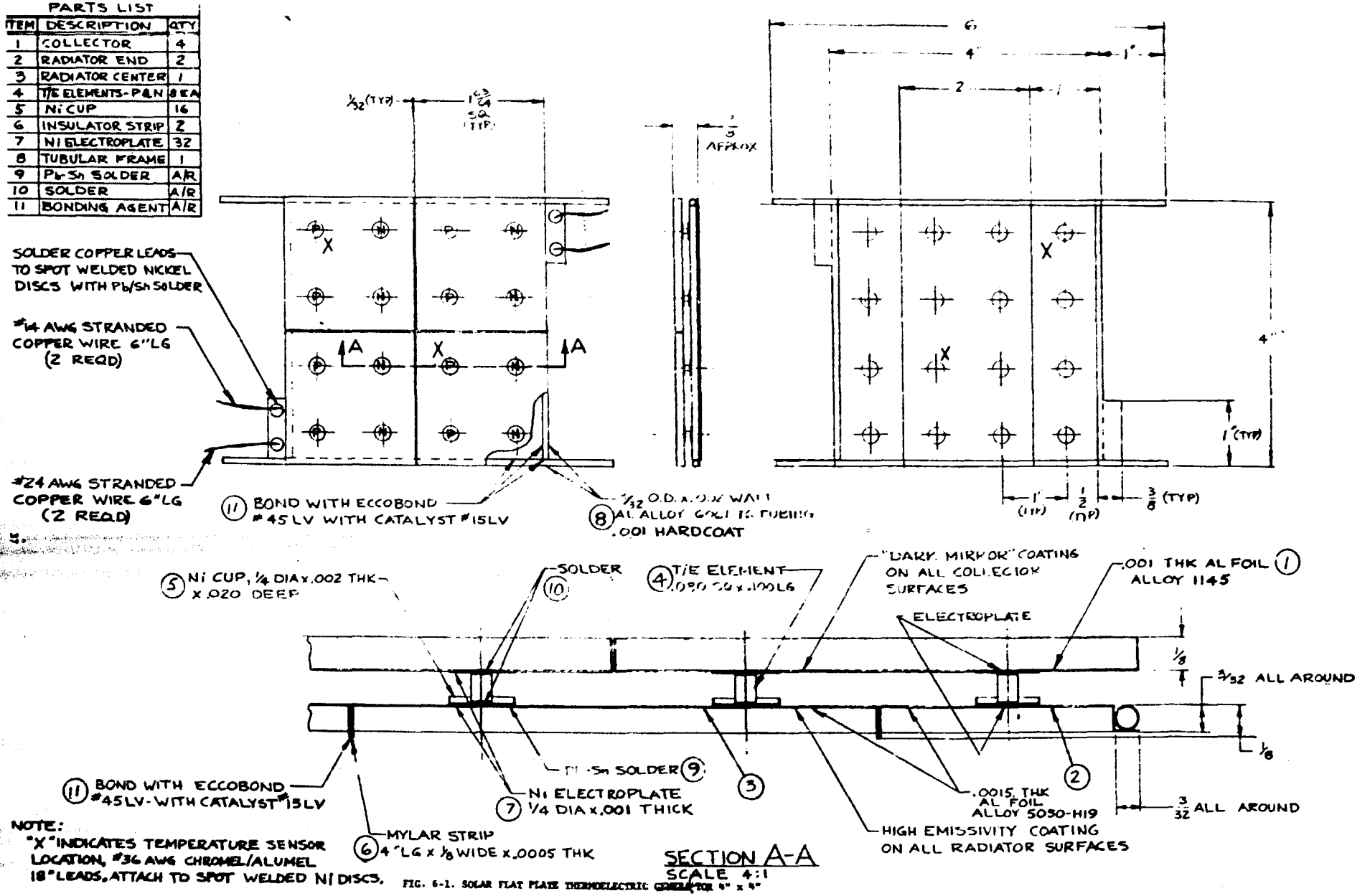

NOTE:
"X" INDICATES TEMPERATURE SENSOR LOCATION, #36 AWG CHROMEL/ALUMEL 18" LEADS, ATTACH TO SPOT WELDED Ni DISCS.

FIG. 6-1. SOLAR FLAT PLATE THERMOELECTRIC GENERATOR 6" x 6"

PARTS LIST		
ITEM	DESCRIPTION	QTY
1	COLLECTOR	36
2	RADIATOR SAW	2
3	RADIATOR CENTER	18
4	RADIATOR END	1
5	TUBULAR FRAME	
6	T/E ELEMENT-PAN	7/14
7	N CUP	144
8	N.E.P. PLATE	288
9	INSULATOR STRIP	A/R
10	SOLDER	A/R
11	Pb-Sn SOLDER	A/R
12	BONDING AGENT	A/R

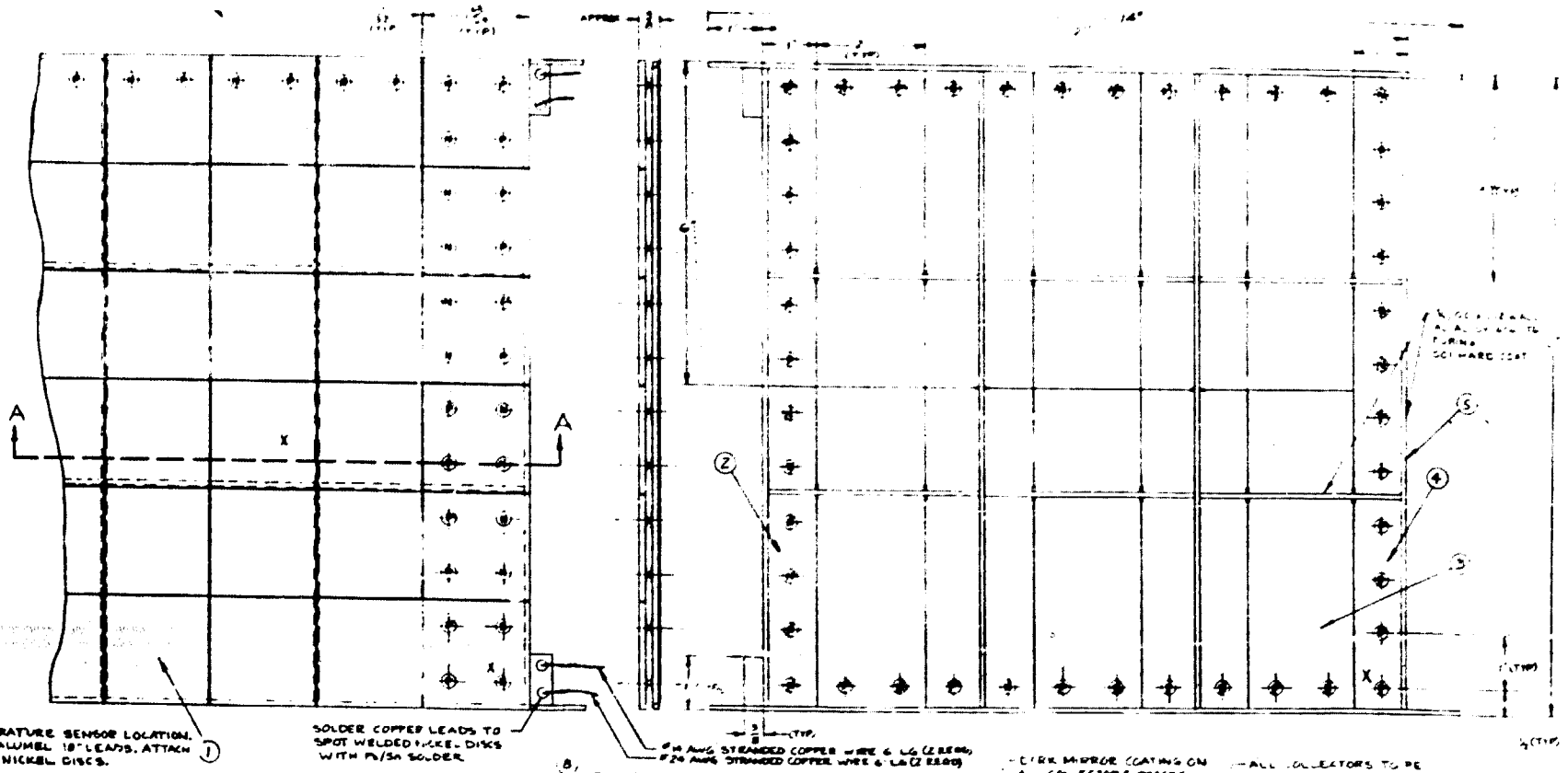

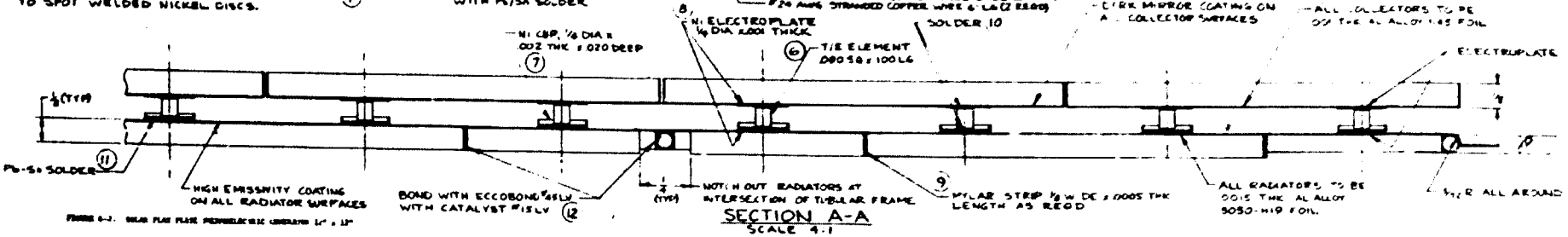

SECTION A-A
SCALE 4:1

PARTS LIST

No.	DESCRIPTION	QTY.
1	T/E ELEMENT	36
2	RADIATOR END	2
3	RADIATOR CENTER	10
4	RADIATOR END	1
5	TUBULAR FRAME	1
6	T/E ELEMENT-P&N LEG	72
7	Ni CUP	144
8	Ni ELECTROPLATE	288
9	INSULATOR STRIP	A/R
10	SOLDER	A/R
11	Pb-Sn SOLDER	A/R
12	BONDING AGENT	A/R

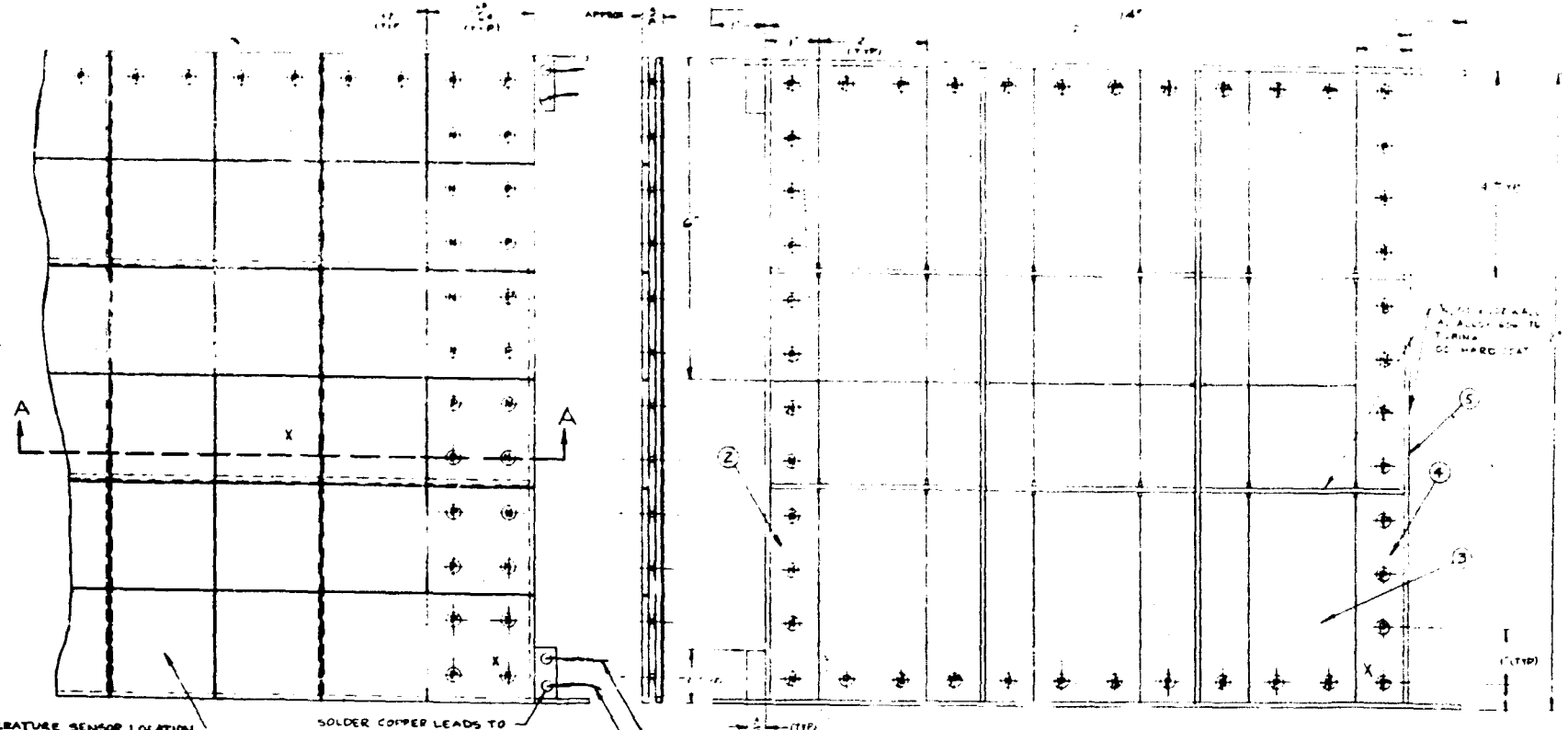

NOTE
"X" INDICATES TEMPERATURE SENSOR LOCATION. #36 AWG CHROMEL/ALUMEL 18" LEADS, ATTACH (1) TO SPOT WELDED NICKEL DISCS.

SOLDER COPPER LEADS TO SPOT WELDED NICKEL DISCS WITH Pb/Sn SOLDER

#14 AWG STRANDED COPPER WIRE 6" LG (2 REQD)
#24 AWG STRANDED COPPER WIRE 6" LG (2 REQD)

SILVER MIRROR COATING ON ALL COLLECTOR SURFACES

ALL COLLECTORS TO BE .0015 THK AL ALLOY 1145 FOIL

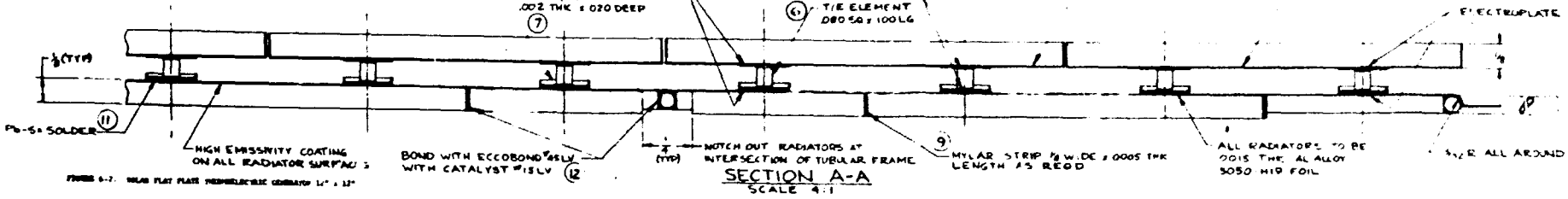

SECTION A-A
SCALE 4:1

FIGURE 6-2. SOLAR FLAT PLATE THERMOELECTRIC GENERATOR 12" x 12"

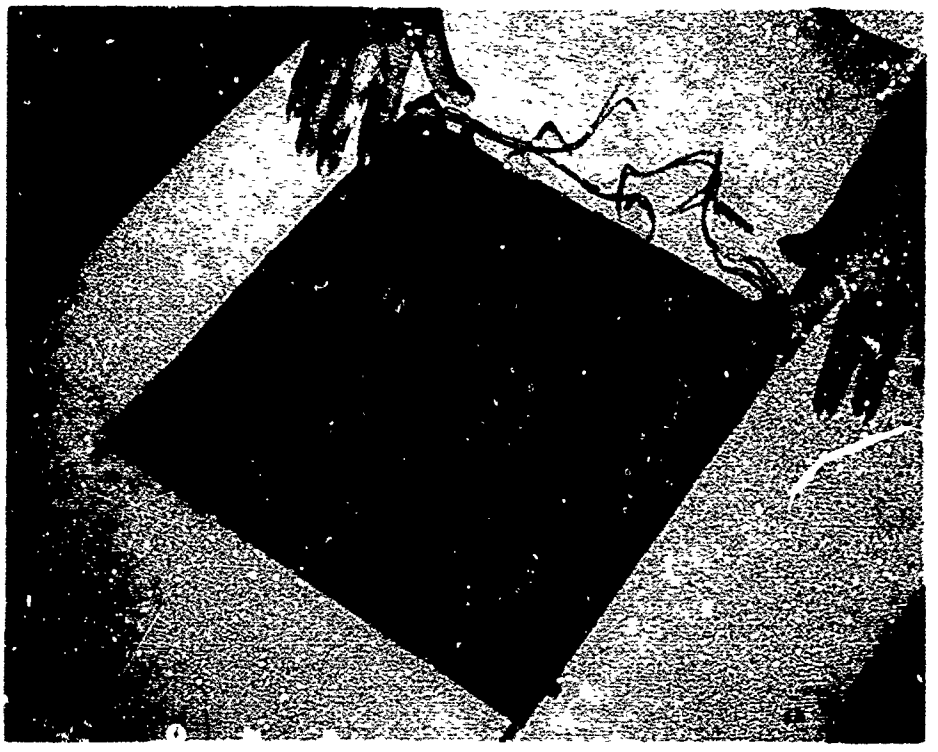

SOLAR FLAT PLATE THERMOELECTRIC GENERATOR 12" X 12"

FIGURE 6-3

Table 6-1 presents a weight analysis, based on measurements, for a 12" x 12" panel. The panel weight at present is 53.4 grams per square foot, exclusive of temperature sensors, power wires and voltage wires.

TABLE 6-1

Weight Analysis For the Solar Flat Plate Thermoelectric Generator

Component	gms/ft^2
Thermoelectric material	10.0
Nickel electroplate or radiator and collectors	1.6
Solder, thermoelement to nickel	7.4
Cups	2.9
.001" aluminum collector plate	6.5
Collector support structure	3.9
.0015" radiator plate	9.7
Radiator support structure	2.0
Solder (radiator side, metal to metal)	1.8
Hard coated aluminum support tubes	2.8
Epoxy cement	4.8
Temperature sensors	2.0
TOTAL	55.4
TOTAL, less temperature sensors	53.4

Rather straightforward development may be able to reduce this weight by 1.5 to 2.0 grams per square foot by allowing the use of lower solder weights and less cement. A major weight reduction could occur if the element length were decreased but this requires development effort.

7. PROTOTYPE PANEL TESTING

7.1 Performance

In accordance with contract requirements, a total of three panels, two 4" x 4" and one 12" x 12", were assembled as described in Section 6. These panels were assembled into the test apparatus schematically depicted in Figure 7-1. The apparatus consisted of an evacuated bell jar containing a heat sink cooled by liquid nitrogen and a set of four incandescent lamps comprising the heat source. Each test panel was suspended between the source and the sink and the enclosure was evacuated to 2 x 10^{-5} torr.

Two thermal cycles were imposed upon each panel, a cycle consisting of 55 minutes on/35 minutes off. At least two hot junction temperature readings and two cold junction temperature readings were taken at the end of each "on" period. The panel was connected across a matched load so that open circuit voltage, closed circuit voltage and current could be measured at the end of each "on" period. The data is tabulated in Table 7-1.

Certain comments can be made concerning this data:

1. The problem of non-uniform heat flux was severe--especially with the 12" x 12" panel.

2. The liquid nitrogen cooling was less effective with sample PB-5 than it was with the other two test articles.

3. When the panel power output is corrected to the theoretical operating temperature difference then sample PB-6 would develop 1.1 watts and sample PB-5 would develop 1.36 watts. This latter value is close to the corrected power outputs measured for other panels tested. This calculation is subject to some error depending on how closely the average of the installed temperature sensors reflected the actual average temperature difference across the panel.

4. The differences in developed power between successive runs for PB-5 and PB-6 are readily explained by small temperature changes.

7.2 Sinusoidal Vibration Testing

In accordance with contract requirements, a total of three panels*, two 4" x 4" and one 12" x 12" were subjected to the following sinusoidal vibration test:

Test in each axis proceeding at a single sweep at a constant octave rate from the lower to the upper frequency limit in not less than 45 minutes.

*PB-1, PB-5, PB-6

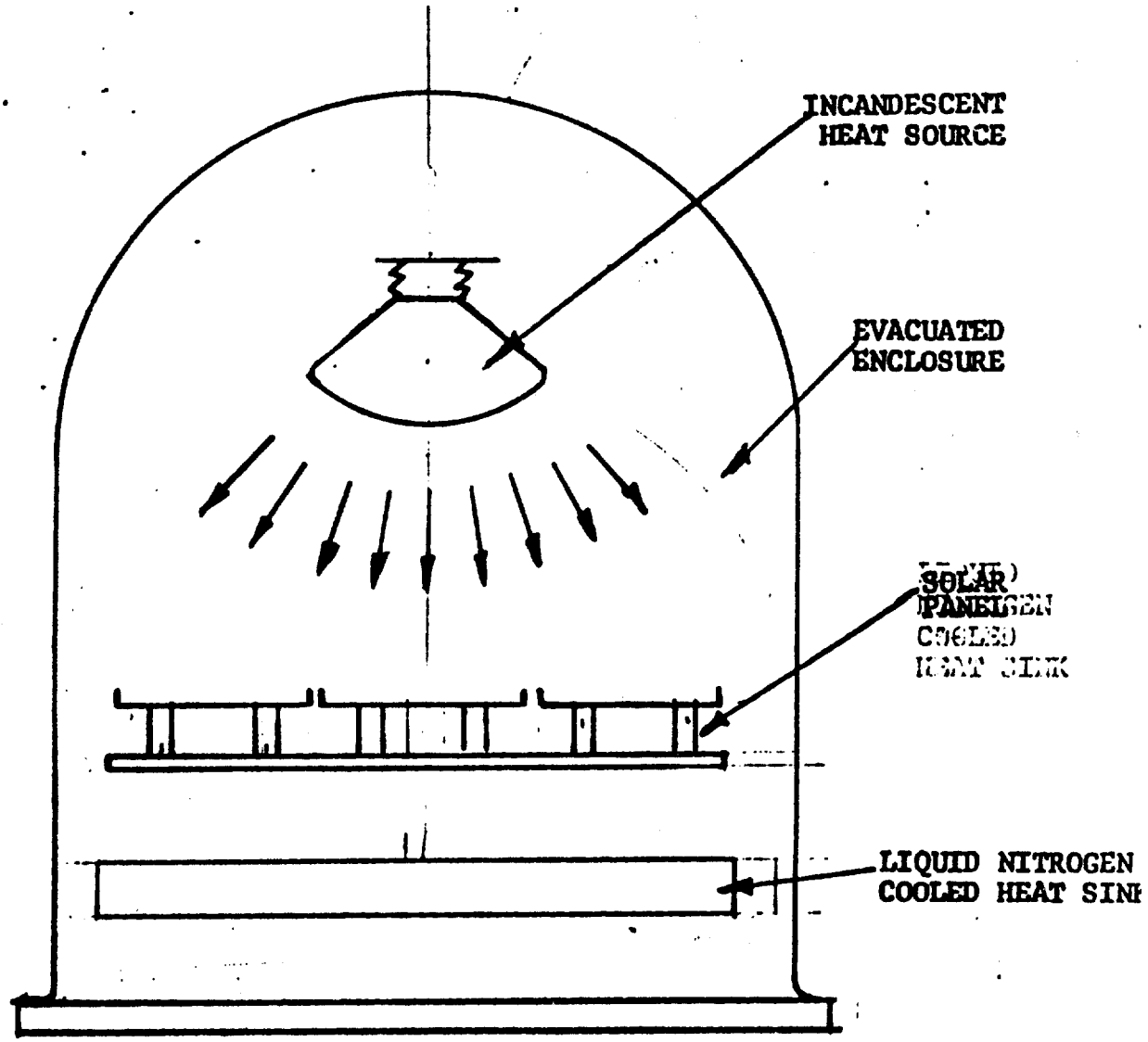

FIGURE 7-1

PANEL PERFORMANCE TEST APPARATUS - SCHEMATIC

TABLE 7-1. PANEL PERFORMANCE TEST DATA

	Panel No. PB-1 12" x 12"		Panel No. PB-5 4" x 4"		Panel No. PB-6 4" x 4"	
	Cycle 1	Cycle 2	Cycle 1	Cycle 2	Cycle 1	Cycle 2
Hot Junction Temperature 1	159°C	162°C	216°C	216°C	236°C	235°C
" " " 2	240°C	237°C	231°C	231°C	209°C	207°C
" " " 3	164°C	167°C	-	-	-	-
Cold " " 1	70°C	74°C	114°C	117°C	90°C	92°C
" " " 2	93°C	97°C	117°C	117°C	84°C	92°C
Open Circuit Voltage, Volts	.38	.38	.064	.063	.074	.072
Closed Circuit Voltage, Volts	.18	.18	.032	.0315	.037	.036
Current, amperes	3.9	3.9	2.51	2.49	2.7	2.64
Output Power, watts	.7	.7	.081	.078	.101	.095
Watts/square foot	.7	.7	.73	.70	.91	.85

Frequency, cps	Amplitude	'G' Loading
5-14	0.5" double amplitude	-
14-40	-	5
40-400	-	7.5
400-3000	-	15

The testing was performed on a Model C-10 electromechanical shaker manufactured by the MB Electronics Company.

In the sinusoidal vibration test the panel was mounted to a fixture by using the aluminum support tubes. The tubes were clamped on the portion extending beyond the converter area proper. This applies also to the random vibration, the acceleration and the shock tests.

The resistance of each panel was measured before and after each sweep in each axis. No resistance change was detected on any panel. Certain resonant frequencies in the collector panels were noted as follows:

Panel	Resonant Frequencies With Panel Horizontal
PB-1	70, 140, 290 cps
PB-5	140 cps
PB-6	130, 240 cps

No visual evidence was observed of any panel damage due to this vibration testing.

7.3 Random Vibration Testing

This test was conducted by Associated Testing Laboratories, Inc., Wayne, New Jersey and is documented by their report J231-4707. The test required random vibration along each axis, white noise with an amplitude of $0.05g^2$ per cycle per second from 15 to 2000 cps for 5 minutes. The equipment used can be listed as follows:

Vibration Exciter	Ling Electronics Corp. Model 275
Power Cubicle	" Model PP-60/100 VO-1
Remote Control Console	Ling Electronics Corp. Model 102-(1001-1)
Random Noise Control Console	Ling Electronics Corp. Model R-1001-3

Resistance measurements made before and after each run on each of the three panels* indicated no change. Visual examination of each panel at the completion of each axis of vibration revealed no evidence of physical damage.

*PB-1, PB-5, PB-6

7.4 Acceleration Testing

The three panels were subjected to an acceleration test of 12 "g" for 10 minutes in each of the three mutually perpendicular axes. The testing was performed by Associated Testing Laboratories on their Model AC-10,000 radial accelerator and is documented by their report J231-4707.

No changes in electrical resistance or appearance were detected due to this testing.

7.5 Shock Testing

This test requires that three shocks of 40 g's each for 6 milliseconds be applied in each of the three mutually perpendicular axes of each of the three panels. The test was performed on an Avco Shock Machine, Model SM-005, using a PK 015 pad calibrated by Avco on March 20, 1964.

No changes in electrical resistance or appearance were detected due to shock testing.

7.6 Thermal Cycling Test

This test requires that one 12" x 12" panel and one 4" x 4" panel be subjected to 500 thermal cycles of 55 minutes on/35 minutes off each and that temperatures and power output be measured on a daily basis. The test was performed in the apparatus schematically depicted in Figure 7-1 with the exception that water cooling was used rather than liquid nitrogen.

The panels were connected to a matched load and power output was determined by measuring current and voltage drop across the load. The data for the 12" x 12" panel, PB-1, is given in Table 7-2. The data for the 4" x 4" panel, PB-6, is given in Table 7-3.

As discussed above, Section 7-1, the 12" x 12" panel (PB-1) was subjected to a very non-uniform heating. This caused a considerable uncertainty in the relationship between measured panel power output and the panel power output in operational conditions. The stability of the measured power output, see Table 7-2, is considered satisfactory, however.

The stability of the 4" x 4" panel, PB-6, was less satisfactory. A gradual reduction in power output took place during the test, see Table 7-3, resulting in a total reduction of about 25%. About 9% of this change is a result of a panel resistance increase. The remainder is a result of a decrease in panel voltage. When the 500 cycles were completed, the panel was examined and one open element was found. This would account for about 6% of the resistance change of 9%. When the panel was removed from the test apparatus a second open element was found. It is reasonable to suppose that this second element was partially open during the test, thereby accounting for the balance of the resistance change. No explanation can be offered for the voltage decrease.

TABLE 7-2

Cycling Test Results For Panel PB-1

Vacuum: 2×10^{-5} Torr. Cycle: 1 hour on/1/2 hour off Panel Size 12" x 12"

No. of Cycles	Hot Junction Temperature °C (Average)	Cold Junction Temperature °C (Average)	Power Output Watts/ft^2	Power Output Watts/ft^2 Corrected*
16	174	76	.528	1.19
48	177	72	.563	1.10
64	174	79	.577	1.25
128	179	79	.573	1.24
160	177	80	.550	1.27
176	179	81	.572	1.29
192	178	80	.574	1.29
240	174	80	.545	1.33
256	177	82	.547	1.31
272	174	81	.558	1.39
304	179	83	.530	1.24
352	180	83	.562	1.28
368	180	83	.561	1.28
384	178	82	.535	1.25
400	180	84	.563	1.32
416	177	82	.558	1.34
512	179	84	.552	1.32

*Corrected to theoretical temperature difference of 147°C. Correction performed by assuming that power output is proportional to the square of the temperature difference.

TABLE 7-3

Cycling Test Results For Panel PB-6

Vacuum: 10^{-5} Torr. Cycle: 1 hr. on/1/2 hr. off Panel Size: 4" x 4"

No. of Cycles	Hot Junction Temperature °C (Average)	Cold Junction Temperature °C (Average)	Power Output Watts	Power Output Watts/ft^2	Power Output Watts/ft^2 Corrected*
16	221	97	.101	.909	1.20
48	225	98	.105	.945	1.25
64	227	97	.102	.918	1.17
128	225	96	.094	.846	1.10
160	225	94	.095	.855	1.06
176	222	94	.093	.837	1.10
192	228	96	.095	.855	1.06
240	227	95	.093	.837	1.03
256	230	97	.094	.846	.98
272	227	94	.094	.846	1.03
304	226	92	.092	.828	1.00
352	231	95	.091	.819	.96
368	229	96	.093	.837	1.02
384	232	100	.091	.819	1.01
400	234	100	.088	.792	.96
416	231	101	.087	.783	1.00
512	232	100	.081	.729	.90

*Corrected to theoretical temperature difference of 147°C. Correction performed by assuming that power output is proportional to the square of the temperature difference.

8. OPERATIONAL ANALYSIS

The results of this research program can be broadly stated as follows: with respect to panel weight and reliability the results were more than satisfactory, with respect to efficiency the results were distinctly disappointing. In this section, an analysis will be made of the expected performance in orbit of the panels fabricated under this program. It is also of interest, however, to evaluate the performance of panels incorporating certain specific improvements. Before doing this, it is important to investigate the reasons why the efficiency of the prototype panels was unsatisfactory and what improvements might be made.

The reasons why the delivery panel efficiency was low can be listed as follows:

(a) The efficiency of the collector coating used was only 80% that initially expected.

(b) The efficiency of the basic thermoelectric material available for prototype panels was only 78% of that initially expected.

(c) The efficiency of the micro-thermoelements used in prototype panels was only 84% of the efficiency of the basic thermoelectric material.

(d) After assembly into the panels a loss in Seebeck voltage occurred (for reasons not presently known) which resulted in the thermoelements having an additional 25% efficiency loss.

(e) Another 10-15% power loss occurs due to either (1) variations in thermoelement properties or (2) uneven heating of the thermoelements.

For convenience, two basic classes of technological improvements will be defined. Class I, an improvement requiring distinct materials or/and process developments and advances. Class II, an improvement that can be expected by straightforward engineering procedures.

Items (a) and (b) in the list above are considered to require Class I improvements in order to achieve an efficiency increase. Items (c), (d) and (e) are considered to require Class II improvements in order to achieve an efficiency increase.

The performance at present is only 30-35% of that initially predicted. The Class II improvements would increase this to 60%.

The overall efficiency initially predicted was 3.8% or 5 watts/ft^2. It is now realized that if both the collector coating and the thermoelectric materials performed exactly as predicted, only 4-4.5 watts/ft^2 would be achieved because of sheet electrical resistance losses in the radiator and collector plates. The actual value would depend on sheet thickness and a trade-off between efficiency and weight is indicated.

The performance test data for the solar flat plate panels, 12" x 12" size, is open to considerable doubt because of the uncertainty relative to heat flux uniformity (see Section 7.1). The data for 4" x 4" panels is more representative of the performance power to be expected under uniform heating. This indicates a power output of about 1.3-1.4 watts/square foot. Class II improvements could increase this to 2.3 to 2.6 watts/sq. foot. Class I improvements could increase this to 3.5-4 watts/square foot. Table 8-1 presents this efficiency data and specific power data.

TABLE 8-1

Panel Efficiency and Specific Power

Status	Watts/sq. ft.	Watts/lb.
Present	1.3-1.4	11-12
Class II improvements	2.3-2.6	20-22
Class I improvements	3.5-4	30-34

Cost is an operational factor of considerable interest. A cost estimate has been made for the fabrication of sufficient thermoelectric solar panels to provide over one killowatt of power. It was assumed that some additional development work would precede such fabrication.

The cost estimates given in Table 8-2 assume that one system per year would be produced. The costs are for panels only and do not include deployment or orientation mechanism.

TABLE 8-2

Solar Flat Plate Cost Estimate

System Power Level	Dollars Per Watt
2-3 kw.	$31.90
6-7 kw.	26.00
15-18 kw	22.10
27-30 kw.	20.00

9. THERMAL STORAGE EVALUATION

9.1 Design

A space vehicle in a 300 mile Earth orbit will be in the Sun approximately 55 minutes and in shadow approximately 35 minutes for each orbit. It will be assumed, for the purposes of this discussion, that the space vehicle has a continuous requirement for electrical power. If the source of electrical power is a solar energy converter, then a requirement exists to store energy during the sunlight period for use during the Earth shadow period. It has been customary to use electrochemical batteries for such storage. It is the purpose of this analysis to examine storing energy in the form of heat in conjunction with a solar flat plate thermoelectric generator. Since this system has certain growth possibilities, it is of interest to examine thermal storage with respect to existing technology and with respect to certain state-of-art advancements.

Storage Mechanism Selection

A number of natural phenomena can be considered for the thermal storage of energy. These may be generally categorized as follows:

(a) The heat capacity of a substance undergoing temperature changes.

(b) Substances that utilize the heat of vaporization.

(c) Substances that utilize the heat of fusion.

Since phase change transformation will almost always store more energy per unit mass than the heat capacity of a material and since constant temperature operation is very desirable for a thermoelectric converter, (a) above can be eliminated from further consideration. The use of the heat of vaporization (b) has two principal drawbacks. The vapor must go through a considerable volume change at constant pressure. This implies a collapsible container, and a mechanism to maintain constant force on the container. Even if a vapor can be found with a suitable condensing pressure, the containment vessel would undoubtably add considerable weight, especially if meteorite protection were added. In addition, vapors are generally poor heat conductors, so that evaporation would occur from the vessel surface. If, in the process of evaporation, droplets are separated from the mass, there is, in the absence of gravity, no force available to bring them back to it. Each time they approach the wall, they will encounter a flow of vapor away from it which would tend to keep them floating in the center of the vessel. This could result in dry spots developing and over-heating, which, if they do not burn through, would radiate abnormal quantities of heat and decrease the efficiency of the generator.

The heat of fusion (c) is the most promising of the mechanisms that have been considered. Since the vapor pressure of many substances is very low at their melting point and since specific volume changes that

occur in going from the solid to the liquid phase are relatively small, the problem of containing a melting solid is much less difficult than that of containing an evaporating liquid.

Storage Material Selection

The criteria that have been established for storage material selection are; (a) melting temperature, (b) heat of fusion (in BTU per pound), (c) specific power of the system in watts per pound, and (d) weight of thermal storage material container.

A previous study (3) indicated that a melting temperature in the range 300°F and 500°F would be desirable for the thermoelectric materials and optical coatings suitable for solar flat plates. Table 9-1 presents a list of the candidate materials, their heats of fusion and melting temperatures. If the specific power in watts per pound for solar flat plate thermoelectric converters with thermal storage is calculated, the heat of fusion of lithium is found to be the most suitable storage mechanism (3).

System Thermal Analysis

The sketch below illustrates the thermal inputs and outputs of a solar flat plate with energy storage.

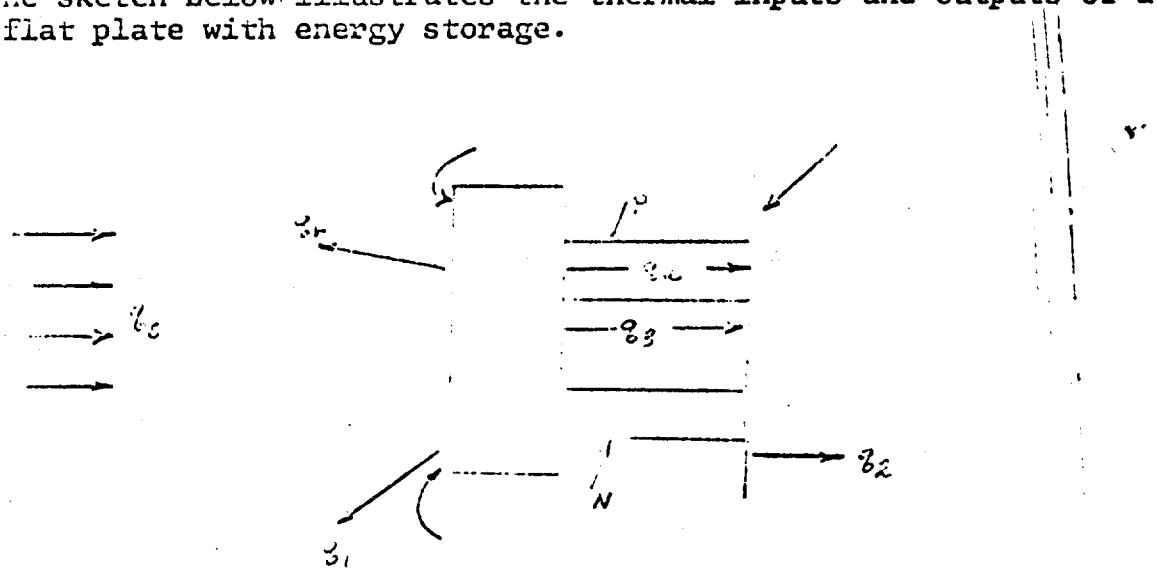

q_s = solar flux
q_r = reflected heat
q_1 = re-radiated heat
q_a = heat available for conversion
q_3 = intra-plate radiation
q_2 = heat rejected from radiator

FIGURE 9-1. RESISTANCE OF MATERIALS TO LIQUID LITHIUM

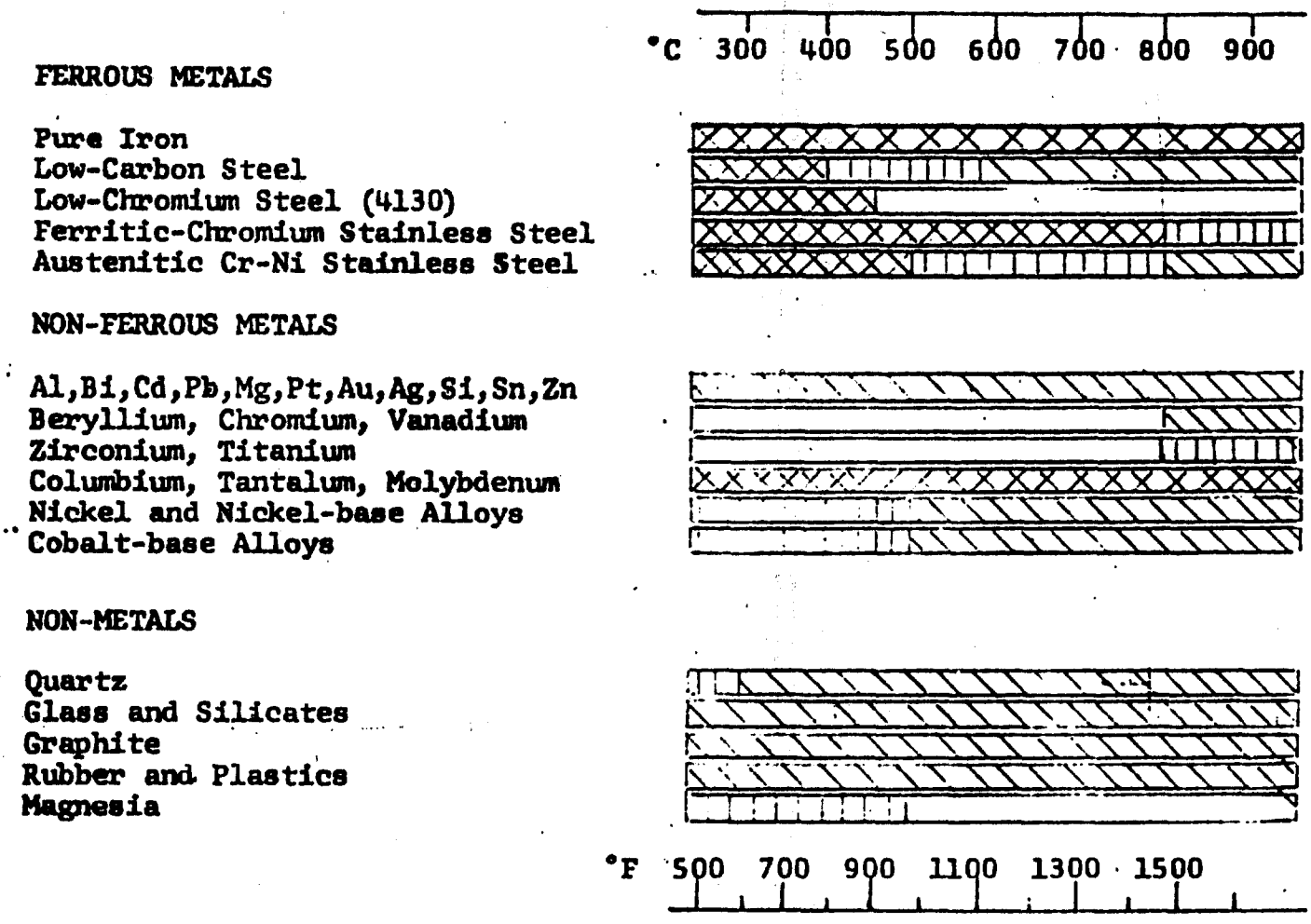

Resistance Ratings:

These ratings refer to liquid-metal resistance only -- not to temperature, dependent mechanical strength of metallurgical stability.

- Good - Consider for relatively long-time use.
- Limited - Short-time use only.
- Poor - No structural possibilities.
- Unknown - Information inadequate.

R. N. Lyon, Ed., "Liquid-Metals Handbook", 2d Ed. Rev., Supt. of Documents, Washington, D. C., 1954.

Since a heat of fusion mechanism is used for thermal storage, the collector (hot junction) temperature is constant with time. Since the thermoelectric converter represents a fixed thermal resistance; q_a, q_3, q_2 and the radiator (cold junction) temperature are all invariant with respect to time. Due to the fixed collector temperature, q_1 does not vary with time.

The heat through the converter, q_2 or $q_3 + q_a$, is fixed with respect to time. The heat into the thermal storage material, $q_s - q_r$, is of course introduced only during the 55 minute sunlit period. The thermal input into the storage material, $q_s - q_r$ is effectively equalized with respect to time by the storage material and a time invariant thermal input can be defined by multiplying $q_s - q_r$ by the ratio of sunlit time to total time:

$$(q_s - q_r)_{\text{time invariant}} = (q_s - q_r)_t$$

$$(q_s - q_r)_t = (q_s - q_r)\ 55 \text{ minutes}/90 \text{ minutes}$$

The time invariant thermal input into the thermoelectric converter is thus equal to, $(q_s - q_r)_t - q_a$. Since q_a is radiated at a constant temperature (melting point of lithium) from a known emissivity surface it can be evaluated. The intra plate radiation q_3, can be readily evaluated knowing intra plate emissivities and plate temperatures, thus enabling q_a, heat available for conversion to be determined. Once $(q_s - q_r)_t$ is known, it can be combined with the heat of fusion data for lithium and the amount of lithium required can be calculated.

Knowledge of hot and cold junction temperatures and the thermoelectric properties of the materials used allows the thermoelectric efficiency to be calculated which in turn allows the panel output power to be determined.

A mathematical analysis of the solar flat plate, based on the discussion, is given in Appendix A-1 together with the solution of a sample problem.

The Containment Problem

There are several mechanisms through which liquid metals, such as lithium, may attack container materials. Lithium uses all these mechanisms. Firstly, the molten lithium can actually dissolve the container material forming a liquid solution. This situation is severe as the rates of corrosion are usually quite rapid. Secondly, a direct alloying in the solid state can take place between the lithium and the container material. As this mode of corrosion depends on solid state diffusion, it is slower and, hence, less severe. Thirdly, and particularly in the case where the chosen container material is a complex alloy, a selected leaching of the

container by the lithium, in the molten state, may take place.

Thus, it can be seen from the large variety of corrosion modes, that the problem of containing liquid lithium must be studied. Fortunately, a literature search has revealed several promising materials for our application. Figure 9-1 summarizes some data on the corrosion resistance of a number of materials to lithium as a function of temperature (5). This table represents a good guide for selecting a container material. The terms good, limited and poor are defined as follows:

Term	Rate of Attack
Good	$<.001$"/year
Limited	$<.01" > .001$"/year
Poor	$>.01$"/year

It can be seen from Figure 9-1, that pure iron has good resistance to attack by lithium. Furthermore, the ferrite chromium stainless steels have better corrosion resistance to lithium than the austenitic chromium nickel stainless steels. "Among the non-ferrous metals, not all of which are listed on the chart, aluminum, barium, bismuth, calcium, cadmium, gold, lead, magnesium, platinum, silicon, silver, strontium, thallium, tin and zinc, all have poor corrosion resistance to lithium. They react with lithium to form compounds that have no structural value." It is important to note that the data compiled in Figure 9-1 represents a number of sources and reports where both static and dynamic testing was carried out. Thus, on the basis of this compiled evidence, pure iron has been chosen as a candidate container material.

More recent information (6) indicates that titanium, .004" thick wall, will contain lithium for a three year mission. Because the density of titanium is only 57.5% that of iron, a significant weight saving is obtained.

Weight Analysis

A weight analysis of solar flat plate panels with thermal storage, has been made based on the assumptions listed in Table 9-2. The assumptions are given both for the current state-of-art in panel fabrication and upon certain improvements, both in thermoelectric material and in optical coatings, that are considered reasonable.

The results of this analysis, both current and improved systems, are given in Table 9.3. Because the advanced system assumes a higher collector absorptivity than is presently available, thereby collecting more energy, a greater weight of storage material is required for the improved system.

Performance Study

The results of the thermal analysis and the weight analysis have been combined to calculate panel performance indices for both current and

TABLE 9-1

Survey of Candidate Thermal Storage Materials

Material	Melting Point °C	Heat of Fusion Calories/gram.
	179	104
$Bi(NO_3)_3$	261	88.5
$LiHSO_4$	170.5	-
$MgCl_2KCl_6H_2O$	265	-
$HgBr_2$	237	11.0
$HgCl_2$	277	15.3
Al_2Cl_6	192	63.2
As_2S_3	300	-
As_4O_6	274	30.1
Bi	270	12.2
$BiCl_3$	230	8.2
H_2BO_3	185	-
$Cd(C_2H_3O_2)_2$	256	-
$MoCl_5$	194	-
KNO_3	297	33.4
$KHSO_4$	210	-
$K_2S_2O_7$	300	-
$AgNO_3$	212	18
$NaNH_2$	210	-
$NaClO_3$	248	50.7
$NaNO_3$	310	-
$NaNO_2$	271	44.7
		54.0
Na_2S_4	275	-
Na_2S_5	251	-
NaCNS	287	55.0
Sn	231	14.6
$ZnCl_2$	275	40.4

TABLE 9-2

Assumptions That Form the Basis of the Weight Analysis

Sunlit Period	Θ_s = 55 minutes
Shadow Period	Θ_D = 35 minutes
Solar Flux	q_s = 130 watts/ft^2
Mission Time	3 years
Thermal Storage Material	Lithium
Storage Material Container	Iron or titanium
Thermoelectric Material	Bismuth telluride, p and n
Figure of Merit	Z; 1.9×10^{-3} °C^{-1} (Present)
	2.4×10^{-3} °C^{-1} (Future)
Collector Absorptivity	α; 0.82 (Present)
	0.9 (Future)
Collector Emissivity	e_1; 0.08 (Present)
	0.05 (Future)
Radiator Emissivity	e_2; 0.9 (Present)
	.95 (Future)

TABLE 9-3

A Weight Tabulation of a Solar Flat Plate With Thermal Storage

Item	#/ft^2 Current State-of-Art		#/ft^2 Advanced State-of-Art	
	Titanium	Iron	Titanium	Iron
Lithium storage material	.69	.69	.76	.76
Storage container	.20	.35	.20	.35
Aluminum radiator plate (.004" thick)	.06	.06	.05	.06
Thermocouple Assemblies	.11	.11	.13	.13
Support structure	.10	.10	.10	.10
TOTAL	1.16	1.31	1.25	1.40

TABLE 9-4

Performance Indices For a Solar Flat Plate With Thermal Storage

Index	Current State-of-Art		Advanced State-of-Art		% Improvement of Advanced System
	Titanium	Iron	Titanium	Iron	
Watts/ft^2 (Cont.)	2.05	2.05	2.81	2.81	37
Watts/# of system (Continuous)	1.76	1.56	2.25	2.0	27
# of system/watt (Continuous)	.57	.64	.44	.50	
$\frac{\text{Watt-hours}}{ft^2 - \text{cycle}}$	3.07	3.07	4.2	4.2	37
$\frac{\text{Watt-hours}}{\# - \text{cycle}}$	2.57	2.34	3.37	3.0	27

improved systems. These indices are presented in Table 9-4. It is of interest to note, that the advanced system yields a greater improvement in efficiency, watts/square foot, than in specific power, watts/pound.

9.2 Testing

Objective of Experiment

The object of this experiment was to test the feasibility, in a simulated space environment, of the thermal storage concept associated with solar heated thermoelectric flat plate generators.

Procedure

The storage pad, itself, was fabricated by sealing a 1 1/2" x 1 1/2" x 1/4" pre-shaped lithium block in a .004" thick type 304 Stainless steel container. With the use of a thin layer of epoxy cement, a bismuth telluride thermocouple assembly was attached to the storage package while suitable temperature sensors were placed at the heat collecting surface and at thermoelement hot and cold junctions.

The system described above was mounted in an evacuated bell jar equipped with a radiant heat source. In order to increase the absorptivity of the collecting surface of the storage container, a graphite coating was applied to its surface. The system was subjected to a thermal cycle consisting of 12 minutes off, and 28 minutes on.

Discussion of Results

The numerical results of this experiment are summarized in Table 9-5. Temperature measurements on the pad during the test showed only a 2°C difference across the entire lithium thickness. Thus, the power producing thermocouple hot junction remained essentially at the melting point of lithium, 179°C. It may have been noted that the off time of this test cycle, corresponding to the time required to completely solidify the lithium, is lower than the specified orbit dark period of 35 minutes. This reduction in dark period time may be explained by the fact that a non-selective, high emissivity coating was used on the collecting surface, permitting large radiation losses. Except for this alteration in cycle period the system functioned very well. The hot junction temperature remained constant throughout the entire orbit, indicating that the storage mechanism was supplying its latent heat of fusion during the dark period. Furthermore, the bismuth telluride thermocouple output voltage and internal resistance remained constant. This situation prevailed for more than 20 operating cycles when the test was discontinued and all objectives were met.

This test was considered successful to the extent that thermal storage was demonstrated. The dark time capacity was, however, considerably less than the desired 30 minutes. This was believed due to excessive collector losses.

Subsequent to the above experiment the test unit was re-worked by cementing aluminum foil, incorporating a spectrally selective coating to the collector side of the storage container.

This unit was assembled in the apparatus described above and a test was performed. The storage time increased but only to 16 minutes. The reason for the poor performance is not known. The test could not be repeated because the test apparatus was required for thermal cycling testing of contractual delivery items.

TABLE 9-5

Numerical Results of the Thermal Storage Feasibility Test

Collector Temperature °F	354
Hot Junction Temperature °F	350
Radiator Temperature °F	230
Dark Time Capacity - minutes	12
Light Phase Time - minutes	28
Number of Cycles Tested	20

10. CONCLUSIONS AND RECOMMENDATIONS

The solar flat plate thermoelectric generator has been successfully developed with respect to the following criteria:

(a) Light Weight

The present weight of less than 55 grams per square foot represents an advanced state of weight reduction for this component. Further significant weight reduction can be obtained only by using shorter thermoelements, which requires a major development program, or by using larger area thermoelements on a greater intra-element spacing. Since the increased spacing results in greater electrical and thermal losses, the improvement in grams/square foot is limited.

(b) Environmental Integrity

Panels have successfully passed thermal cycling sinusoidal and random vibration, shock, and acceleration tests.

(c) Ease of Fabrication

The specific panel design utilized allows low cost fabrication due to simplified assembly procedures and minimal material costs.

The units developed under this program were, however, less satisfactory with respect to conversion efficiency.

This reduced performance can be attributed to the following factors:

(a) The spectrally selective collector coating is less efficient than had been predicted. An improvement in this coating of up to 20% can be anticipated. The Air Force is presently conducting research in this general area.

(b) The thermoelectric material presently available is less efficient than had been anticipated. If materials were to be developed having properties more suitable to the flat plate operating temperature regime an efficiency increase of 20% or more is possible.

(c) Processing of the elements into solar flat plate assemblies results in an additional 25% loss for reasons not presently known.

The performance degrading factors listed above must be improved before the solar flat plate thermoelectric generator can be seriously considered as a useful space power source. If such improvements can be achieved, a further set of problems requires investigation. These concern the erection, deployment and orientation of large area converters. The actual system weight will depend to a large extent upon the solution to these problems.

An analysis and limited test program has demonstrated the feasibility of thermal energy storage, contemplating the replacement of electrochemical storage. A further systems analysis is required to determine those missions where thermal storage might be applicable.

The following recommendations can be made. These recommendations are intended to guide further development leading to improved solar flat plate thermoelectric generators.

(a) Develop improved collector coatings useful in the temperature range 200-250°C.

(b) Develop thermoelectric materials optimized for the temperature range 100-230°C.

(c) Develop processing techniques for fabricating and assembling thermoelements, approximately 2cm x 2cm x 2.5cm long, without degradation in figure of merit.

(d) If improvements are made in the above areas, then an investigation of deployment and orientation problems should be initiated.

11. BIBLIOGRAPHY

1. Flat Plate Solar Thermoelectric Conversion Panels, ASD-TDR-62-214, May, 1962.

2. Flat Plate Solar Thermoelectric Generator Orbital Experiment, ASD-TDR-63-479, May, 1963.

3. Proposal to the United States Air Force For Solar Flat Plate Thermoelectric Generator Research, KN-142, September 14, 1962, General Instrument Corporation.

4. Semiconductor Thermoelements and Thermoelectric Cooling, A. F. Ioffe, 1957, Infosearch, London.

5. Lithium Corporation of America, Bulletin 104-257.

6. The Effect of Molten Alkali Metals on Containment Metals and Alloys at High Temperatures, DMIC, Battelle Memorial Institute, Columbus, Ohio.

APPENDIX A-1

THERMAL ANALYSIS*

Solar Flat Plate With Thermal Storage

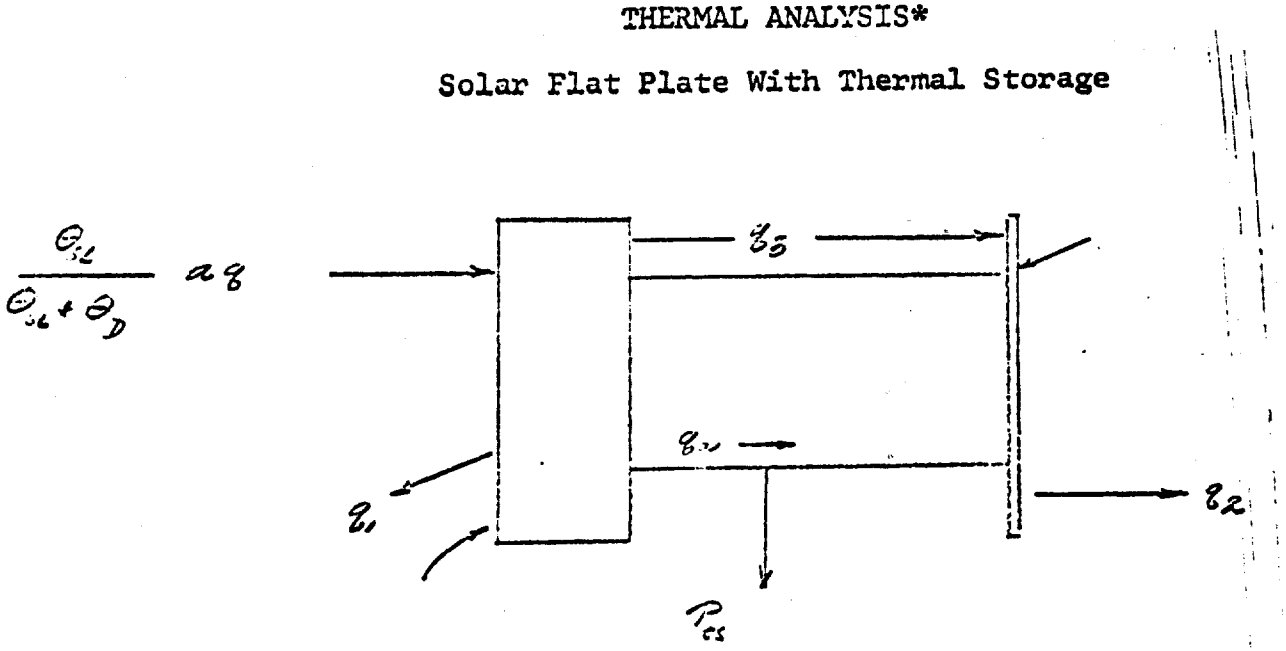

Find: P_{ts}, continuous per square foot of panel

Assume: 1. Thermal storage design adequate to maintain T_H and T_C constant

2. Thermal storage utilizes the heat of fusion of lithium

3. Assume radiation to absolute zero

Analysis:

1. If T_H and T_C are constant, q_1, q_3, q_a, q_2, and P_{ts} are all constant

2. If all of the energy received by the system per cycle is utilized at a constant rate then we can define an average thermal power input as:

$$\frac{\theta_{SL}}{\theta_{SL} + \theta_D} \cdot a_q$$

3. T_H is known from the melting point of lithium, so that q_1 can be determined:

$$q_1 = \alpha \epsilon_{11} (T_H)^4$$

*See Nomenclature

4. $\frac{\theta_{s2}}{\theta_{s2}+\theta_3} \cdot a q = q_1 + q_2 + P_{ts}$ (heat balance)

5. Since P_{ts} is less than 5% of the heat throughput it will be neglected hereafter.

6. $q_2 = \frac{\theta_{s2}}{\theta_{s2}+\theta_3} \cdot (a q - q_1)$

7. $q_2 = \sigma e_c T_c^4$ so that T_C can now be determined

8. $q_3 = q_2 - q_a$ (heat balance)

$$q_3 = \frac{\sigma e_3}{2 - e_3} (T_H^4 - T_c^4)$$

q_3 can therefore be determined, and in turn, q_a

9. From materials information, knowing T_H and T_C, Z can be determined.

10. Knowing T_H, T_C, and Z, $N_{T/E}$ can now be determined from

$$N_{T/E} = \frac{T_H - T_c}{T_H} \cdot \frac{\quad}{\quad}$$ (See reference 3)

11. $P_{ts} = N_{T/E} \; q_a / 3.41 \; \frac{\text{BTU/hour}}{\text{Watt}}$

Sample Calculation

12. Given: $a = \quad$ $e_3 = 0.05$ θ_{s2} = 55 minutes

$e_H = 0.08$

$e_c = 0.9$ $\theta_3 =$ minutes

$q =$ $\frac{\text{BTU/hour}}{\text{ft}^2}$ $T_H = 816°R$ (melting point of lithium)

Find: P_{ts}

13. $aq\left(\frac{\theta_{sc}}{\theta_{sc}+\theta_{\infty}}\right) = 222$ BTU/hour/ft^2 (from 2)

14. $q_1 = .171(0.02)\left(\frac{816}{100}\right)^4 = 61$ BTU/hour/ft^2 (from 3)

15. $q_2 = 222 - 61 = 161$ BTU/hour/ft^2 (from 6)

16. $T_{c_1} = \sqrt[4]{161/.171(0.9)}$ (from 7)

$T_C = 570°R$

17. $q_3 = \frac{.171(.05)}{2-.05}\left[(816/100)^4 - (570/100)^4\right]$

$= 15$ BTU/hour/ft^2

18. $q_a = q_2 - q_3 = 161-15 = 146$ BTU/hour-ft^2 (from 8)

19. From materials data $Z = 1.9 \times 10^{-3}\ °C^{-1} = 1.05 \times 10^{-3}\ °F^{-1}$

20. $m = \sqrt{1 + \frac{.00105}{2}(816+570)} = 1.31$ (from 10)

21. $N_{T/E} = \frac{816-560}{816} \cdot \frac{1.31-1}{1.31 + \frac{560}{816}}$ (from 10)

$= .31 \cdot \frac{.31}{2.0} = 4.78\%$

22. $P_{ts} = .0478 \times 146/3.41 = 2.05$ watts/ft^2 continuous (from 11)

23. $E = \frac{2.05 \text{ watt } (1.5 \text{ hr/cycle})}{\text{ft}^2} = \frac{3.07 \text{ watt-hrs}}{\text{ft}^2\text{-cycle}}$

APPENDIX A-1

Calculation of Weight of Lithium Required

The amount of lithium required, per square foot of panel, is that amount which is sufficient to supply the energy requirements of the panel during the shadow portion of the cycle.

= heat of fusion of lithium, 187.6 BTU/#

= pounds of lithium required per square foot

24. $\lambda w = (q_2 + q_1)\,\theta_D \left(\frac{1 \text{ hour}}{60 \text{ minutes}}\right)$

Sample calculation

25. From 24 $\lambda w = (q_1 + q_2)\,\theta_D$

From 15 $q_2 = 161$ BTU/hr/Ft^2, $q_1 = 61$, $61 + 161 = 222$ BTU/hr-ft^2

$\theta_D = 35$ min/60 min/hr.

187.6 BTU/#(w) = 222 BTU/hr-ft^2 x 35/60 min-hr/min.

w = 0.69 #/Ft^2 of lithium

Since the specific gravity of lithium = 0.53 the thickness of lithium required,

$$L = \frac{.69\ \#/ft^2}{.53(62.4\ \#/ft^3)} = .0237 = .46''$$

NOMENCLATURE

Item	Description	Units
a	Absorptivity of collector	Dimensionless
e_H	Emissivity of collector	Dimensionless
e_c	Emissivity of radiator	Dimensionless
e_3	Intra-plate emissivity	Dimensionless
-	Thickness of lithium storage material	Inches
m	Resistance ratio	Dimensionless
q	Solar flux	BTU/hour-ft^2
q_1	Re-radiated heat	BTU/hour-ft^2
q_r	Reflected heat	BTU/hour-ft^2
q_2	Heat rejected by radiator	BTU/hour-ft^2
q_3	Intra-plate radiation	BTU/hour-ft^2
q_a	Heat available for conversion	BTU/hour-ft^2
T_H	Hot junction temperature	°R
T_C	Cold junction temperature	°R
P_{ts}	Converter power output, continuous	Watt/ft^2
E_{ts}	Converter energy output, per cycle	Watt-hours / ft^2 - cycle
W	Amount of lithium required	$\frac{\text{Pounds}}{\text{ft}^2}$
Z	Thermoelectric figure of merit	°C^{-1}
$N_{T/E}$	Thermoelectric efficiency	Dimensionless
λ	Heat of fusion	BTU/#
Θ_D	Shadow time	Minutes
Θ_{sl}	Sunlit time	Minutes
α	Stefan Boltzman constant	BTU/(sq.ft)(hr)(°R)^4